Eur. Phys. J. C 56, 39–55 (2008)
DOI 10.1140/epjc/s10052-008-0641-3

THE EUROPEAN PHYSICAL JOURNAL C

Regular Article – Theoretical Physics

Survival probability for diffractive Higgs production in high density QCD

J. Miller[a]

Department of Particle Physics, School of Physics and Astronomy, Raymond and Beverly Sackler Faculty of Exact Sciences, Tel Aviv University, Ramat Aviv, Tel Aviv, 69978, Israel

Received: 23 November 2006 / Revised version: 7 January 2008 /
Published online: 18 June 2008 –

Abstract. In this paper, the contribution of hard processes described by BFKL pomeron exchange is taken into account by calculating the first enhanced diagram. The survival probability is estimated, using the ratio of the first enhanced diagram and the single pomeron amplitude, taking into account all essential pomeron loop diagrams in the toy model of Mueller. The triple pomeron vertex is calculated explicitly in the momentum representation. This calculation is used for estimating the survival probability, and it turns out that the survival probability is small, at 0.4%. Hard pomeron rescattering processes contribute substantially to the survival probability.

1 Introduction

1.1 The survival probability

The goal of this paper is to calculate the survival probability, taking into account the contribution of hard processes described by BFKL pomeron exchange. Diffractive Higgs production is a typical hard process, in which the Higgs is produced from the one parton shower due to gluon fusion. This process can be calculated in perturbative QCD.

The signature of this process is the existence of so called large rapidity gaps (LRG), in which no particles are produced [1, 2]. For the LHC energies and for diffractive Higgs production at c.m. rapidity equal to zero, there are two rapidity gaps. The first is between the right moving final protons and the Higgs boson, the second is between the left fast moving proton and the Higgs boson.

As was noticed by Bjorken [2], in hadron–hadron collisions there is a considerable probability that more than one parton shower can be produced. Therefore, one needs to suppress such a multi-parton shower production, since it can produce particles that fill up the rapidity gap. This suppression can be characterized by the survival probability [2, 3].

To illustrate what survival probability is, it is instructive to calculate it in the simple eikonal model for soft pomerons. 'Soft pomeron' means that there are no perturbative contributions from short distances, and only soft non-perturbative processes contribute to the high energy asymptotic behavior. The survival probability is defined in the eikonal formalism as [2, 3]

$$\langle|S^2|\rangle = \frac{\int |\mathcal{M}(s,b)|^2 \mathrm{e}^{-\Omega(b)}\,\mathrm{d}^2b}{\int |\mathcal{M}(s,b)|^2\,\mathrm{d}^2b}\,, \tag{1}$$

where $\mathcal{M}$ is the amplitude for the hard process under consideration, in impact parameter space (where b is the impact parameter), at the center of mass energy $\sqrt{s}$. In this paper, this is the amplitude of diffractive Higgs production from one parton shower. $\mathrm{e}^{-\Omega(b)}$ gives the probability that additional inelastic scattering will not occur between the two partons at impact parameter b. $\Omega(b)$ is called the opacity or optical density. Therefore, the numerator is the amplitude for the exclusive process, while the denominator is the same process, due to the exchange of one pomeron.

The survival probability was estimated in [4], in the eikonal approach for exclusive central diffractive production at the LHC. The survival probability here was given for the process illustrated in Fig. 1 in terms of the impact parameter b. Generally, in all these models the survival probability is given by the expression

$$\langle|S^2|\rangle = \frac{\int \mathrm{d}^2b_1\,\mathrm{d}^2b_2\left(A_{\mathrm{H}}(b_1)A_{\mathrm{H}}(b_2)(1-A_{\mathrm{s}}((b_1+b_2))^2)\right)^2}{\int \mathrm{d}^2b_1\,\mathrm{d}^2b_2(A_{\mathrm{H}}(b_1)A_{\mathrm{H}}(b_2))^2}; \tag{2}$$

$A_{\mathrm{H}}(b)$ is the hard pomeron amplitude in impact parameter space b shown in Fig. 1. The amplitude $A_{\mathrm{H}}\,(b)$ for hard pomeron exchange can be calculated in perturbative QCD and is responsible for the production of two gluon jets, with BFKL ladder gluons between them (see Fig. 1). In this model [4], the hard pomeron in Fig. 1 emits the Higgs boson. $A_{\mathrm{H}}(b)$ is given in the impact parameter b represen-

[a] e-mail: jeremymi@post.tau.ac.il, leving@post.tau.ac.il

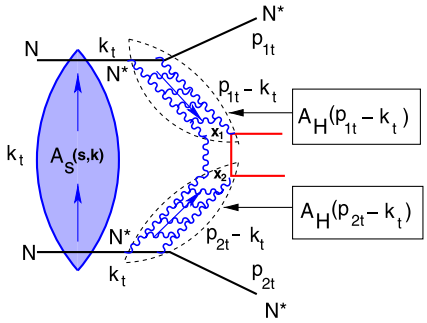

Fig. 1. Central diffractive production in the two channel eikonal model in proton scattering due to pomeron exchange

tation by the expression [4]

$$A_{\mathrm{H}}(b) = \frac{1}{\pi R_{\mathrm{H}}^2} \mathrm{e}^{-\frac{b^2}{R_{\mathrm{H}}^2}}, \tag{3}$$

$R_{\mathrm{H}}^2 = 7.2\,\mathrm{GeV}^{-2}$. As shown in Fig. 1, $A_{\mathrm{H}}(b_1)$ and $A_{\mathrm{H}}(b_2)$ denote the hard pomeron amplitude above and below the Higgs signal respectively. The contribution A_{s}, shown in Fig. 1, denotes the soft pomeron amplitude. $(1 - A_{\mathrm{s}})$ includes all possible initial state interactions due to the exchange and interaction of soft pomerons. $(1 - A_{\mathrm{s}})$ also includes the possibility that the two initial nucleons in Fig. 1 do not interact at all.

The survival probability was found to be 5%–6% for the single channel model. In the two channel model, the survival probability here is 2.7% at the LHC energy of $\sqrt{s} = 14\,000\,\mathrm{GeV}$. The upper bound for the survival probability, in the constituent quark model (CQM), was found to be 6.0%–0.1% at the LHC energy. This is almost the same as the survival probability found in the single channel model. The two upper bounds intercept at an energy just above the typical LHC energy. This suggests that the upper bound for the survival probability should be 2%–3% for measurements at the LHC.

The first attempt to estimate the contribution of hard (semi-hard) processes to the value of the survival probability was made by Bartels et al. in [5]. They considered the contribution of this "fan" pomeron diagram to the value of the survival probability, and they found that this contribution is rather large. Namely, the value ranges from 3.17% for $\alpha_{\mathrm{s}} = 0.15$, to 1.6% for $\alpha_{\mathrm{s}} = 0.25$, (where α_{s} is the QCD coupling).

The aim of this paper, is to calculate the BFKL pomeron (see Fig. 4) and the first enhanced diagram for the BFKL pomeron (see Fig. 7). These calculations are in the symmetric QCD dipole approach. Because in proton–proton scattering, there is no reason to assume that the mean field approximation, based on the "fan" diagram, can work. The ratio of the two contributions of Figs. 4 and 7 are calculated and used to estimate the value of the survival probability.

This paper is organized in the following way. In Sect. 2, the coupling of the BFKL pomeron to the color dipole (Sect. 2.1) and the triple pomeron vertex (Sect. 2.2) are calculated in the momentum representation. Using these results, the BFKL pomeron amplitude shown in Fig. 4 is calculated (Sect. 2.3), and the first enhanced diagram shown in Fig. 7 is calculated (Sect. 2.4).

Section 3 is devoted to the survival probability, estimated in the QCD dipole approach. The ratio of the two contributions of Figs. 4 and 7 is calculated, which is used to estimate the value of the survival probability (Sect. 3.2). It turns out that this ratio is not small, and this indicates the importance of taking into account all enhanced diagrams. Therefore, in Sect. 3.3, all enhanced diagrams are summed in the toy model [6]. The fact that the two dipoles have different sizes is neglected. From the calculation of the ratio of Figs. 4 and 7, the value of the parameter d of this model is determined (d is the low energy amplitude for one pomeron exchange). Using this parameter, the value of the survival probability was estimated as the ratio of the diffractive Higgs production in this model and Higgs production in one parton shower (for single pomeron exchange). It turns out that the survival probability is rather small.

In the conclusion, the results for the value of the survival probability are presented. A discussion is given of the dependence of the value of the survival probability on the choice of the intercept of the BFKL pomeron. The significance of higher order hard rescattering contributions to the survival probability is also discussed.

2 The conformal eigenfunctions of the vertex operator and the triple pomeron vertex

All calculations are carried out in the momentum representation, and the strategy and notation of [11] is closely followed. Firstly, the pomeron coupling to the QCD color dipole is introduced (see Fig. 2) in the momentum representation. Secondly, an explicit expression for the triple pomeron vertex (see Fig. 3) is derived. Using both these formulae, the BFKL pomeron (Fig. 4) and the first enhanced diagram (Fig. 7) are calculated in the symmetric QCD dipole approach.

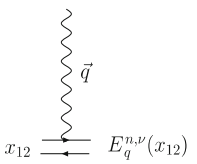

Fig. 2. The interaction vertex of pomeron with the dipole

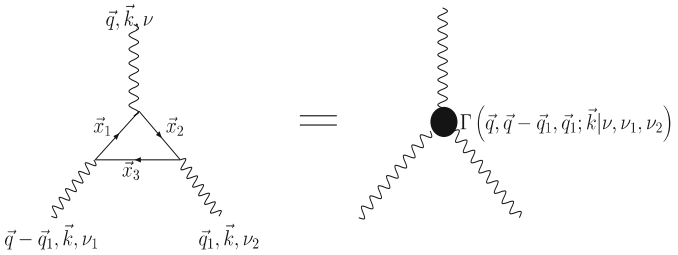

Fig. 3. The triple pomeron vertex

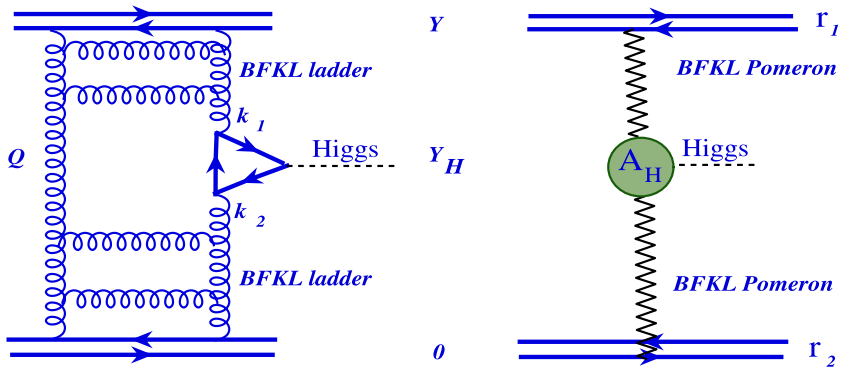

Fig. 4. Central diffractive production in color dipole scattering due to single pomeron exchange

2.1 The BFKL pomeron vertex function

The vertex coupling the BFKL pomeron to the couple dipole is illustrated in Fig. 2. Here, $\mathbf{q}$ is the momentum transferred along the pomeron, and $\mathbf{x}_{12}$ is the transverse size of the dipole. In the notation of [7–10], the eigenfunctions for the vertex in coordinate space are defined as

$$E^{n,\nu}(x_{01},x_{20}) = (-1)^n \left(\frac{x_{10}x_{20}}{x_{12}}\right)^{\gamma} \left(\frac{\bar{x}_{10}\bar{x}_{20}}{\bar{x}_{12}}\right)^{\bar{\gamma}}, \quad (4)$$

where $x_{ij} = x_i - x_j$ and x_i are the transverse coordinates. The conformal dimensions are defined as

$$\gamma = \frac{n+1}{2} + \mathrm{i}\nu\,, \quad \bar{\gamma} = -\frac{n-1}{2} + \mathrm{i}\nu\,, \quad (5)$$

n is the conformal spin, and it is an integer. The energy levels of the pomeron are the BFKL eigenvalues given by [7]

$$\omega(n,\nu) = \bar{\alpha}_{\mathrm{s}}\chi(\gamma) = \bar{\alpha}_{\mathrm{s}}(2\psi(1) - \psi(\gamma) - \psi(1-\gamma))\,, \quad (6)$$

where in this paper the notation

$$\bar{\alpha}_{\mathrm{s}} = \frac{\alpha_{\mathrm{s}}N_c}{\pi} \quad (7)$$

is used, and where $\psi(f) = \mathrm{d}\ln\Gamma(f)/\mathrm{d}f$ and $\Gamma(f)$ is the Euler gamma function. Since the only intercept $\omega(n=0,\nu)$ is positive at high energies, the contribution with $n \neq 0$ can be neglected. Lipatov in [7] introduces the following mixed representation of the vertex:

$$E_q^{n,\nu}(\mathbf{x}) = \frac{2\pi^2}{b_{n,\nu}}\frac{1}{|\mathbf{x}|}\int \mathrm{d}^2R \mathrm{e}^{\mathrm{i}\mathbf{q}\cdot\mathbf{R}} E^{n,\nu}\left(R+\frac{x}{2}, R-\frac{x}{2}\right), \quad (8)$$

where from [7]

$$b_{n,\nu} = \frac{2^{4\mathrm{i}\nu}\pi^3}{\frac{n}{2}-\mathrm{i}\nu}\frac{\Gamma\left(\frac{n}{2}-\mathrm{i}\nu+\frac{1}{2}\right)\Gamma\left(\frac{n}{2}+\mathrm{i}\nu\right)}{\Gamma\left(\frac{n}{2}+\mathrm{i}\nu+\frac{1}{2}\right)\Gamma\left(\frac{n}{2}-\mathrm{i}\nu\right)}\,. \quad (9)$$

A more convenient expression than (8) for the vertex was calculated in [8–10] and is given as

$$E_q^{n,\nu}(x_{12}) = (qq^*)^{\mathrm{i}\nu}2^{-6\mathrm{i}\nu}\Gamma^2(1-\mathrm{i}\nu) \quad (10)$$
$$\times\left(J_\gamma\left(\frac{q^*x_{12}}{4}\right)J_{\tilde{\gamma}}\left(\frac{qx_{12}^*}{4}\right) - (-1)^n \times J_{-\gamma}\left(\frac{q^*x_{12}}{4}\right)J_{-\tilde{\gamma}}\left(\frac{qx_{12}^*}{4}\right)\right), \quad (11)$$

where J_γ are the Bessel functions of the first kind. In (11), q and q^* are the components of the momentum $\mathbf{q}$ transferred along the pomeron, in the complex representation. That is,

$$|q| = qq^*\,,$$
$$q = q_x + \mathrm{i}q_y\,, \quad q^* = q_x - \mathrm{i}q_y\,. \quad (12)$$

In order to work in the momentum representation when calculating the single pomeron amplitude (Fig. 4), and the first enhanced diagram (Fig. 7), it is necessary to express the vertex function explicitly in the momentum representation. In [11] it was shown that in the momentum representation the vertex function is given by the following Fourier transform:

$$E(\mathbf{p},\mathbf{q};n=0,\gamma) = \frac{b_{n,\nu}}{2\pi^2}\int\frac{\mathrm{d}x}{\sqrt{x}}\exp\left(-\frac{\mathrm{i}p^*x}{2}\right) \times\int\frac{\mathrm{d}x^*}{\sqrt{x^*}}\exp\left(-\frac{\mathrm{i}x^*p}{2}\right)E_q^{n=0,\nu}(x)\,. \quad (13)$$

Here $\mathbf{p}$ denotes the momentum which is the conjugate variable of the dipole size x_{12}. The complex representation, to express the vector $\mathbf{p}$ in terms of its complex components p and p^* (see (12)), is used in (13). In [11], this integral is written in the following factorized form:

$$E(\mathbf{p},\mathbf{q};n=0,\gamma) = \frac{b_{n=0,\nu}}{2\pi^2}(q^2)^{-\mathrm{i}\nu}2^{-6\mathrm{i}\nu}\Gamma^2(1-\mathrm{i}\nu) \times\left\{\tilde{E}(p,q;n=0,\tilde{\gamma})\tilde{E}(p^*,q^*;n=0,\gamma) - \tilde{E}(p,q;n=0,-\tilde{\gamma})\tilde{E}(p^*,q^*;n=0,-\gamma)\right\}, \quad (14)$$

where

$$\tilde{E}(p^*,q^*;n=0,\gamma) = \int\frac{\mathrm{d}x}{\sqrt{x}}J_{n=0,\tilde{\gamma}}\left(\frac{q^*x}{4}\right)\mathrm{e}^{-\frac{\mathrm{i}}{2}p^*x}\,,$$
$$\tilde{E}(p,q;n=0,\tilde{\gamma}) = \int\frac{\mathrm{d}x^*}{\sqrt{x^*}}J_{n=0,\gamma}\left(\frac{qx^*}{4}\right)\mathrm{e}^{-\frac{\mathrm{i}}{2}px^*}\,. \quad (15)$$

At this point, it is assumed that $n=0$, and hence $\gamma = \tilde{\gamma} = -\mathrm{i}\nu$ (see (5)). This is because the only intercept $\omega(n=0,\nu)$ is positive at high energies (see (6)), so the contribution $n \neq 0$ is neglected from now on. Let

$\tilde{E}(p^*,q^*;n=0,\gamma)$ and $\tilde{E}(p,q;n=0,\tilde{\gamma})$ be denoted as $\tilde{E}(p^*,q^*;\nu)$ and $\tilde{E}(p,q;\nu)$ for $n=0$. After integration over x and x^*, the expressions for $\tilde{E}(q,p;\nu)$ and $\tilde{E}(q^*,p^*;\nu)$ are found to be [11]

$$\begin{aligned}\tilde{E}(p,q;\nu) &= \left(\frac{q}{8}\right)^{-\mathrm{i}\nu}(-1)^{-\mathrm{i}\nu}\mathrm{i}^{\mathrm{i}\nu+\frac{1}{2}}2^{\frac{3}{2}-\mathrm{i}\nu}p^{\mathrm{i}\nu-\frac{1}{2}}\frac{\Gamma\left(\frac{1}{2}-\mathrm{i}\nu\right)}{\Gamma(1-\mathrm{i}\nu)}\\ &\times {}_2F_1\left(\frac{1}{4}-\frac{1}{2}\mathrm{i}\nu,\frac{3}{4}-\frac{1}{2}\mathrm{i}\nu,1-\mathrm{i}\nu,\frac{q^2}{4p^2}\right),\\ \tilde{E}(p^*,q^*;\nu) &= \left(\frac{q^*}{8}\right)^{-\mathrm{i}\nu}(-1)^{-\mathrm{i}\nu}\,\mathrm{i}^{\mathrm{i}\nu+\frac{1}{2}}2^{\frac{3}{2}-\mathrm{i}\nu}(p^*)^{\mathrm{i}\nu-\frac{1}{2}}\\ &\times\frac{\Gamma\left(\frac{1}{2}-\mathrm{i}\nu\right)}{\Gamma(1-\mathrm{i}\nu)}\,{}_2F_1\\ &\times\left(\frac{1}{4}-\frac{1}{2}\mathrm{i}\nu,\frac{3}{4}-\frac{1}{2}\mathrm{i}\nu,1-\mathrm{i}\nu,\frac{(q^*)^2}{4(p^*)^2}\right). \quad (16)\end{aligned}$$

Hence, using (16) and the expression for $b_{n=0,\nu}$ in (9), the RHS of (14) can be written in the explicit form of

$$\begin{aligned}E(\mathbf{p},\mathbf{q};\nu) &= -\frac{2^{2+2\mathrm{i}\nu}(p^2)^{\mathrm{i}\nu-\frac{1}{2}}\pi^2}{\nu}\frac{\Gamma^2\left(\frac{1}{2}-\mathrm{i}\nu\right)}{\Gamma^2\left(\frac{1}{2}+\mathrm{i}\nu\right)}\frac{\Gamma(\mathrm{i}\nu)}{\Gamma(-\mathrm{i}\nu)}\\ &\times{}_2F_1\left(\frac{1}{4}-\frac{1}{2}\mathrm{i}\nu,\frac{3}{4}-\frac{1}{2}\mathrm{i}\nu,1-\mathrm{i}\nu,\frac{q^2}{4p^2}\right){}_2F_1\\ &\times\left(\frac{1}{4}-\frac{1}{2}\mathrm{i}\nu,\frac{3}{4}-\frac{1}{2}\mathrm{i}\nu,1-\mathrm{i}\nu,\frac{(q^*)^2}{4(p^*)^2}\right)\\ &+\frac{2^{2-6\mathrm{i}\nu}(p^2)^{\mathrm{i}\nu-\frac{1}{2}}\pi^2}{\nu}\left(\frac{q^2}{p^2}\right)^{2\mathrm{i}\nu}\\ &\times\frac{\Gamma^2(1-\mathrm{i}\nu)\Gamma(\mathrm{i}\nu)}{\Gamma^2(1+\mathrm{i}\nu)\Gamma(-\mathrm{i}\nu)}\\ &\times{}_2F_1\left(\frac{1}{4}+\frac{1}{2}\mathrm{i}\nu,\frac{3}{4}+\frac{1}{2}\mathrm{i}\nu,1+\mathrm{i}\nu,\frac{q^2}{4p^2}\right){}_2F_1\\ &\times\left(\frac{1}{4}+\frac{1}{2}\mathrm{i}\nu,\frac{3}{4}+\frac{1}{2}\mathrm{i}\nu,1+\mathrm{i}\nu,\frac{(q^*)^2}{4(p^*)^2}\right), \quad (17)\end{aligned}$$

where $E(\mathbf{p},\mathbf{q};n=0,\gamma)$ is written as $E(\mathbf{p},\mathbf{q};\nu)$. For single pomeron exchange (see Fig. 4), the conformal spin ν has opposite signs at the two vertices at the ends of the pomeron. In Sect. 2.3, when Fig. 4 is calculated it is assumed that $\mathbf{q}=0$ to simplify the calculation. Hence, from (17), the product of two vertices (for $\mathbf{q}=0$) takes the form

$$E(\mathbf{p},\mathbf{q}=0;\nu)E(\mathbf{p},\mathbf{q}=0;-\nu)=\frac{1}{\nu^2}\frac{16\pi^4}{p^2}. \quad (18)$$

2.2 The triple pomeron vertex

In this subsection the triple pomeron vertex, illustrated in Fig. 3 is calculated explicitly in the momentum representation. It is defined in [8–10, 12, 13] as an integral over the center of mass position vectors (x_{01},x_{02},x_{03}), and the conformal dimensions $(\gamma,\gamma_1,\gamma_2)$ as

$$\begin{aligned}&G_{3P}(\mathbf{q},\mathbf{k},n=0,\gamma,\gamma_1,\gamma_2)=G_{3P}(\mathbf{q},\mathbf{k},\nu,\nu_1,\nu_2)\\ &=\int\frac{\mathrm{d}^2x_{10}\,\mathrm{d}^2x_{20}\,\mathrm{d}^2x_{30}}{x_{12}x_{23}x_{31}}E_q^{n,\nu}(x_{10},x_{20})E_k^{n,\nu_1}(x_{20},x_{30})\\ &\quad\times E_{q-k}^{n,\nu_2}(x_{30},x_{10}). \quad (19)\end{aligned}$$

To calculate the triple pomeron vertex explicitly, the mixed representation of Lipatov in [7] is used for the vertex eigenfunctions $E_q^{n,\nu}$ (see (8)). Note that to simplify the calculation of the first enhanced diagram of Fig. 7, it is assumed that $\mathbf{q}=0$ for the momentum transferred along the pomeron, above and below the pomeron loop. Hence, the triple pomeron vertex shown in Fig. 3 is calculated for $\mathbf{q}=0$. In [13] this mixed representation was used in the definition of (19) to give the expression

$$\begin{aligned}&G_{3P}(\mathbf{q}=0,\mathbf{k},\nu,\nu_1,\nu_2)=\frac{1}{2\pi}\int\frac{\mathrm{d}^2x_{01}}{x_{01}^2}x_{01}^{-2\mathrm{i}\nu-1}\mathrm{e}^{\frac{\mathrm{i}\mathbf{k}\cdot\mathbf{x}_{01}}{2}}\\ &\times\int\mathrm{d}^2x_2\frac{x_{01}^2}{x_{12}^2x_{02}^2}x_{02}^{2\mathrm{i}\nu_1+1}E_k^{n,\nu_1}(x_{02})x_{12}^{2\mathrm{i}\nu_2+1}E_{-k}^{n,\nu_2}(x_{12}). \quad (20)\end{aligned}$$

It is also assumed that $|\nu_1|=|\nu_2|=0$ in evaluating the expression of (20) for the triple pomeron vertex. A complete argument for this assumption is given in Sect. A.2 of the appendix. In brief, the other obvious regions which give a large contribution to the integrals over ν_1 and ν_2, namely the regions close to $\nu_1\to\pm\frac{1}{2}$ $(i=1,2)$, give a vanishing contribution to the first enhanced amplitude, when it comes to integrating over the two rapidity variables Y_1 and Y_2 (see (39)). When evaluating the integrals over ν_1 and ν_2, for the expression of Fig. 7, (see (39)), one expands the BFKL functions $\omega(\nu_1)$ and $\omega(\nu_2)$ around the saddle point $|\nu_1|=|\nu_2|=0$ (see (A.38)), which gives the largest contribution to the integration. In the appendix, the integral of (20) is evaluated to give the triple pomeron vertex as an explicit expression in the momentum representation in (A.15) as

$$\begin{aligned}&G_{3P}(\mathbf{q}=0,\mathbf{k},\nu,\nu_1\to0,\nu_2\to0,)\\ &=k^{\mathrm{i}\nu-\frac{1}{2}}\frac{2^{-2\mathrm{i}\nu}}{4\nu_1\nu_2\pi}\frac{\Gamma^3\left(\frac{1}{2}-\mathrm{i}\nu\right)\Gamma^2(\mathrm{i}\nu)}{\Gamma\left(\frac{1}{2}+\mathrm{i}\nu\right)}. \quad (21)\end{aligned}$$

2.3 The single pomeron amplitude

In this subsection the single pomeron amplitude with Higgs production shown in Fig. 4 is calculated. The two dipoles are separated by a rapidity gap Y, and they have transverse sizes $r_1=x_{12}$ and $r_2=x'_{12}$. The momenta conjugate to the dipole sizes are $\mathbf{p}_1$ and $\mathbf{p}_2$, and $\mathbf{q}$ is the momentum transferred along the pomeron. For simplicity it is assumed that $\mathbf{q}=0$. The single pomeron amplitude with Higgs production, in the QCD dipole approach is denoted $M_{\mathrm{Higgs}}(n=1,Y)$, where Y is the rapidity gap between the two incoming protons, and $n=1$ denotes the single pomeron exchanged between the two protons. In this

notation, the single pomeron amplitude, with Higgs production of Fig. 4, has the expression [7–10, 14, 15]

$$M_{\rm Higgs}(n=1,Y)=P^{\rm BFKL}(\mathbf{p}_1,\mathbf{p}_2,Y,\mathbf{q}=0)A_{\rm H}(\delta Y_{\rm H})\,, \tag{22}$$

where $P^{\rm BFKL}(\mathbf{p}_1,\mathbf{p}_2,Y,\mathbf{q}=0)$ is the single pomeron amplitude given by the expression

$$\begin{aligned}P^{\rm BFKL}(\mathbf{p}_1,\mathbf{p}_2,Y,\mathbf{q}=0)=\frac{\alpha_{\rm s}^2}{4}\oint_C {\rm d}\gamma {\rm e}^{\omega(\gamma)Y}\frac{\left(\gamma-\frac{1}{2}\right)^2}{\gamma^2(\gamma-1)^2}\\ \times E(\mathbf{p}_1,\mathbf{q}=0,n=0,\gamma)\\ \times E(\mathbf{p}_2,\mathbf{q}=0,n=0,\tilde{\gamma})\,.\end{aligned} \tag{23}$$

The contour of integration C is shown in Fig. 5, where C encloses all singularities in the integrand of (23), and the line which goes from $-{\rm i}\infty$ to $+{\rm i}\infty$ stands to the right of all these singularities in the integrand of (23). It is assumed that the integrand vanishes on the semi-circle at infinity shown in Fig. 5, so that it is sufficient to replace

$$\oint_C {\rm d}\gamma \to \int_{-{\rm i}\infty+\epsilon}^{+{\rm i}\infty+\epsilon}{\rm d}\gamma\,. \tag{24}$$

Recall that the definition of the conformal variable γ is $\gamma=(n+1)/2+{\rm i}\nu$, and for the largest contribution one takes the $n=0$ contribution only, for high energies, so that $\gamma=1/2+{\rm i}\nu$. In the variable ν, the limits of integration are $+\infty-{\rm i}\epsilon\geq\nu\geq-\infty-{\rm i}\epsilon$, in the limit that ϵ tends to zero. Hence, in the variable ν, the expression of (23) can be recast in the following form:

$$\begin{aligned}P^{\rm BFKL}(\mathbf{p}_1,\mathbf{p}_2,Y,\mathbf{q}=0)=\frac{\alpha_{\rm s}^2}{4}\int\frac{{\rm d}\nu}{2\pi{\rm i}}\mathcal{D}(\nu){\rm e}^{\omega(\nu)Y}\\ \times E(\mathbf{p}_1,\mathbf{q}=0,\nu)\\ \times E(\mathbf{p}_2,\mathbf{q}=0,-\nu)\,,\end{aligned} \tag{25}$$

where $\omega(n=0,\nu)$ is the solution to the BFKL equation defined in (6), where in the high energy limit one takes $n=0$. From now on the notation $\omega(n=0,\nu)=\omega(\nu)$ is used. $A_{\rm H}(\delta Y_{\rm H})$, which appears in (22), denotes the amplitude of the subprocess which produces the Higgs boson, such as the quark triangle subprocess of Fig. 6. The typical rapidity window which the Higgs boson occupies is

$$\delta Y_{\rm H}=\ln\left(\frac{M_H^2}{4m^2}\right)\,,$$

where m is the mass of the proton. The simplest subprocess with the largest contribution for Higgs production in the standard model is the quark triangle shown in Fig. 6. After the subprocess amplitude of Fig. 6 is contracted with the gluon propagators, the expression for the contribution of the quark triangle shown in Fig. 6 is given by [16, 17]

$$A_{\rm H}(\delta Y_{\rm H})=A\left(M_H^2\right)(\mathbf{k}_1\cdot\mathbf{k}_2)\,, \tag{26}$$

where the factor $A\left(M_H^2\right)$ has the value [18–22]

$$A\left(M_H^2\right)=\frac{2}{3}\left(\frac{-\alpha_{\rm s}\left(M_H^2\right)\left(\sqrt{2}G_{\rm F}\right)^{\frac{1}{2}}}{\pi}\right)\,, \tag{27}$$

where $G_{\rm F}$ is the Fermi coupling. $D(\nu)$, appearing in the single pomeron amplitude of (25), is given by

$$\mathcal{D}(\nu)=\frac{\nu^2}{\left(\nu^2+\frac{1}{4}\right)\,.^2} \tag{28}$$

Assuming that the conjugate momenta $\mathbf{p}_1$ and $\mathbf{p}_2$ of the two scattering dipoles in Fig. 4 are equal in magnitude, (18) can be used for the product of the two pomeron vertices. Hence, (28) can be written as

$$\begin{aligned}&P^{\rm BFKL}(\mathbf{p}_1=\mathbf{p}_2=\mathbf{p},Y,\mathbf{q}=0)\\ &\quad=\frac{4\alpha_{\rm s}^2\pi^4}{p^2}\int\frac{{\rm d}\nu}{2\pi{\rm i}}\frac{1}{\left(\frac{1}{4}+\nu^2\right)^2}{\rm e}^{\omega(\nu)Y}\,.\end{aligned} \tag{29}$$

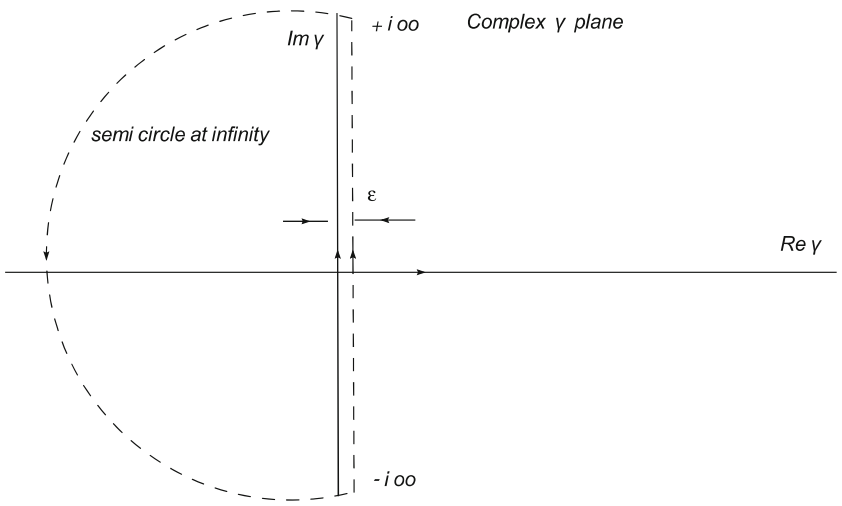

Fig. 5. Contour enclosing singularities for integration over the conformal variable γ

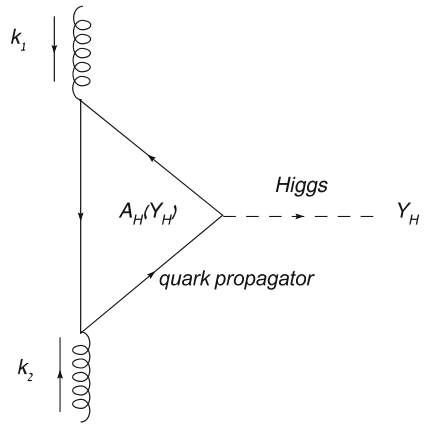

Fig. 6. Quark triangle subprocess for Higgs production

The integration over ν can be evaluated at the saddle point $\nu = 0$ of $\omega\,(\nu)$. In this way, the RHS of (29) becomes

$$P^{\rm BFKL}(\mathbf{p}_1 = \mathbf{p}_2 = \mathbf{p}, Y, \mathbf{q} = 0) = \frac{32\alpha_{\rm s}^2\pi^3}{p^2}\left(\frac{2\pi}{(\omega''(\nu=0)Y)}\right)^{\frac{1}{2}} {\rm e}^{\omega(\nu=0)Y}\,. \qquad (30)$$

Hence, the final expression of (22) for the process of Fig. 4 reads

$$M_{\rm Higgs}(n=1,Y) = \frac{32\alpha_{\rm s}^2\pi^3}{p^2}\left(\frac{2\pi}{(\omega''(\nu=0)Y)}\right)^{\frac{1}{2}} {\rm e}^{\omega(\nu=0)Y} \times A_{\rm H}(\delta Y_{\rm H})\,. \qquad (31)$$

This is the expression for the single pomeron amplitude, including Higgs production, of Fig. 4. However, (31) is written in the approximation that $s = (p_1+p_2)^2 \gg M_H^2$. Since we expect the Higgs mass to be large, we take into account the main correction due to this mass; namely, we make the following replacement:

$$\begin{aligned} {\rm e}^{\omega(\nu=0)Y} &\equiv \left(\frac{s}{m^2}\right)^{\omega(\nu=0)Y} \\ &\longrightarrow \left(\frac{1}{x_1x_2}\right)^{\omega(\nu=0)Y}\left(\frac{4s}{M_H^2}\right)^{\omega(\nu=0)Y} \\ &\equiv {\rm e}^{\omega(\nu=0)(Y-\delta Y_{\rm H})}\,, \end{aligned} \qquad (32)$$

where $\delta Y_{\rm H} = \ln\left(M_H^2/4m^2\right)$ is the typical rapidity window occupied by the Higgs boson, and where m is the mass of proton. x_1 and x_2 are equal to k_1^2/s_1 and k_2^2/s_2 (see Fig. 4) with $s_1 = (p_1+k_1)^2$ and $s_2 = (p_2+k_2)^2$), using the well known kinematic relation $s_1s_2 = M_H^2 s$ and since $k_1^2 = k_2^2 = M_H^2/2$ (see [30] for example). Finally, (31) looks as follows:

$$M_{\rm Higgs}(n=1,Y) = \frac{32\alpha_{\rm s}^2\pi^3}{p^2}\left(\frac{2\pi}{(\omega''(\nu=0)Y)}\right)^{\frac{1}{2}} \times {\rm e}^{\omega(\nu=0)(Y-\delta Y_{\rm H})} A_{\rm H}(\delta Y_{\rm H})\,. \qquad (33)$$

As one can see in (33) the single pomeron exchange does not depend on the value of Higgs boson rapidity ($Y_{\rm H}$) but depends on $\delta Y_{\rm H} = \ln(M_H^2/4m^2)$, which characterizes the window in rapidity occupied by the heavy Higgs boson.

2.4 The first enhanced amplitude

In this subsection the amplitude for the first enhanced amplitude, with Higgs production shown in Fig. 7, is calculated. The pomeron loop is between the two rapidity values Y_1 and Y_2. Hence, one needs to integrate over these two rapidity values. There is also an integral to evaluate, over the unknown momentum $\mathbf{k}$ in the pomeron loop. The enhanced diagram with Higgs production, in the QCD dipole approach is denoted $M_{\rm Higgs}(n=2,Y)$, where $n=2$ denotes

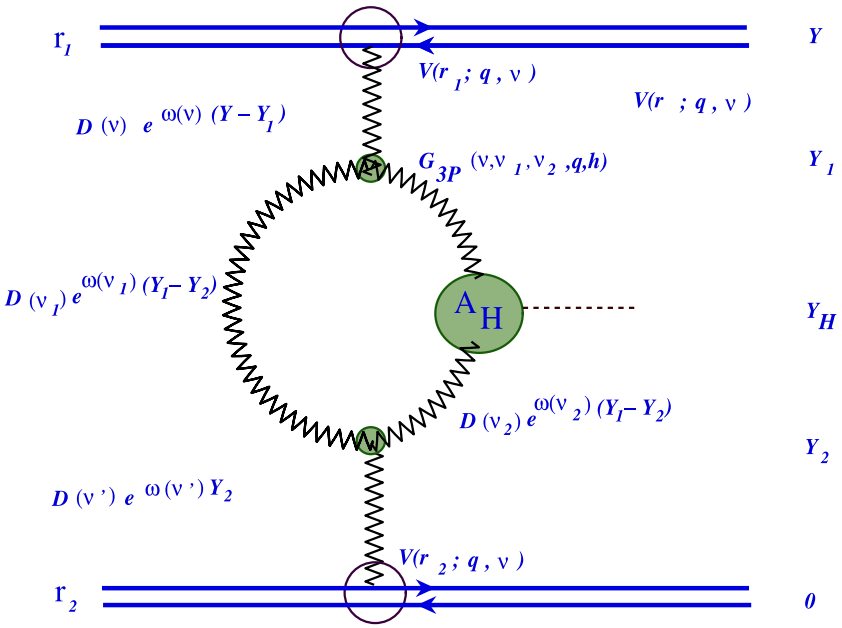

Fig. 7. Central diffractive production in color dipole scattering due to pomeron exchange with a hard rescattering correction

the splitting of the exchanged pomeron, into two branches forming the loop in Fig. 7. The amplitude of Fig. 7, is the first hard rescattering correction, to the single pomeron amplitude of Fig. 4. In this notation, the first enhanced amplitude, with the Higgs production of Fig. 7, is given by

$$M_{\rm Higgs}(n=2,Y)=2P^{\rm BFKL}_{\rm enhanced}(\mathbf{p}_1,\mathbf{p}_2,Y,\mathbf{q})A_{\rm H}(\delta Y_{\rm H})\,, \tag{34}$$

where $P^{\rm BFKL}_{\rm enhanced}(\mathbf{p}_1,\mathbf{p}_2,Y,\mathbf{q})$ is the BFKL pomeron amplitude for the first enhanced one loop diagram, which has the expression given below in (35). The factor of 2 in (34) comes from adding the two identical contributions of Fig. 7, due to the two ways the Higgs boson is emitted from the two branches of the pomeron loop. In order to obtain the complete contribution of Fig. 7, both possibilities for Higgs production from the two branches of the loop must be considered separately and added. $P^{\rm BFKL}_{\rm enhanced}(\mathbf{p}_1,\mathbf{p}_2,Y,\mathbf{q})$ is given by the expression [8–10, 14]

$$\begin{aligned}
&P^{\rm BFKL}_{\rm enhanced}(\mathbf{p}_1,\mathbf{p}_2,Y,\mathbf{q})=\\
&B\oint_C {\rm d}\gamma\oint_{C'}{\rm d}\gamma'\oint_{C_1}{\rm d}\gamma_1\oint_{C_2}{\rm d}\gamma_2\int{\rm d}^2k\int_{Y_{\rm H}+\frac{1}{2}\delta Y_{\rm H}}^{Y}{\rm d}Y_1\\
&\times\int_0^{Y_{\rm H}-\frac{1}{2}\delta Y_{\rm H}}{\rm d}Y_2\\
&\times E(\mathbf{p}_1,\mathbf{q},n=0,\gamma)\frac{\left(\gamma-\frac{1}{2}\right)^2}{\gamma^2(1-\gamma)^2}{\rm e}^{\omega(\gamma)(Y-Y_1)}\\
&\times G_{3P}(\gamma,\gamma_1,\gamma_2,\mathbf{q}=0,\mathbf{k})\\
&\times\frac{\left(\gamma_1-\frac{1}{2}\right)^2}{\gamma_1^2(1-\gamma_1)^2}\frac{\left(\gamma_2-\frac{1}{2}\right)^2}{\gamma_2^2(1-\gamma_2)^2}{\rm e}^{(\omega(\gamma_1)+\omega(\gamma_2))(Y_1-Y_2)-\omega(\gamma_2)\delta Y_{\rm H}}\\
&\times G_{3P}(\tilde{\gamma}',\gamma_1,\gamma_2,\mathbf{q}=0,\mathbf{k})\\
&\times\frac{\left(\gamma'-\frac{1}{2}\right)^2}{\gamma'^2(1-\gamma')^2}{\rm e}^{\omega(\gamma')Y_2}E(\mathbf{p}_2,\mathbf{q},n=0,\tilde{\gamma}')\,,
\end{aligned}\tag{35}$$

$$B=-\frac{\alpha_{\rm s}^4\pi^4}{8}\left(\frac{\alpha_{\rm s}N_c}{2\pi^2}\right)^2\,. \tag{36}$$

The contours of integration C, C', C_1 and C_2 are shown in Fig. 5, where C, C', C_1 and C_2 enclose all singularities in the integrand of (35), and the line which goes from $-{\rm i}\infty$ to $+{\rm i}\infty$ stands to the right of all these singularities in (35). It is assumed that the integrand vanishes on the semi-circle at infinity shown in Fig. 5, so that it is sufficient to replace

$$\begin{aligned}
&\oint_{C'}{\rm d}\gamma\to\int_{-{\rm i}\infty+\epsilon}^{+{\rm i}\infty+\epsilon}{\rm d}\gamma'\,,\quad \oint_{C}{\rm d}\gamma\to\int_{-{\rm i}\infty+\epsilon}^{+{\rm i}\infty+\epsilon}{\rm d}\gamma\,,\\
&\oint_{C_1}{\rm d}\gamma_1\to\int_{-{\rm i}\infty+\epsilon}^{+{\rm i}\infty+\epsilon}{\rm d}\gamma_1\,,\quad \oint_{C_2}{\rm d}\gamma_2\to\int_{-{\rm i}\infty+\epsilon}^{+{\rm i}\infty+\epsilon}{\rm d}\gamma_2\,;
\end{aligned}\tag{37}$$

using the replacements of (37), one can rewrite (35) as

$$\begin{aligned}
&P^{\rm BFKL}_{\rm enhanced}(\mathbf{p}_1,\mathbf{p}_2,Y,\mathbf{q})=B\int_{-{\rm i}\infty+\epsilon}^{+{\rm i}\infty+\epsilon}{\rm d}\gamma\int_{-{\rm i}\infty+\epsilon}^{+{\rm i}\infty+\epsilon}{\rm d}\gamma'\\
&\times\int_{-{\rm i}\infty+\epsilon}^{+{\rm i}\infty+\epsilon}{\rm d}\gamma_1\int_{-{\rm i}\infty+\epsilon}^{+{\rm i}\infty+\epsilon}{\rm d}\gamma_2\int{\rm d}^2k\int_{Y_{\rm H}+\frac{1}{2}\delta Y_{\rm H}}^{Y}{\rm d}Y_1\\
&\times\int_0^{Y_{\rm H}-\frac{1}{2}\delta Y_{\rm H}}{\rm d}Y_2E(\mathbf{p}_1,\mathbf{q},n=0,\gamma)\frac{\left(\gamma-\frac{1}{2}\right)^2}{\gamma^2(1-\gamma)^2}\\
&\times{\rm e}^{\omega(\gamma)(Y-Y_1)}G_{3P}(\gamma,\gamma_1,\gamma_2,\mathbf{q}=0,\mathbf{k})\\
&\times\frac{\left(\gamma_1-\frac{1}{2}\right)^2}{\gamma_1^2(1-\gamma_1)^2}\frac{\left(\gamma_2-\frac{1}{2}\right)^2}{\gamma_2^2(1-\gamma_2)^2}{\rm e}^{(\omega(\gamma_1)+\omega(\gamma_2))(Y_1-Y_2)-\omega(\gamma_2)\delta Y_{\rm H}}\\
&\times G_{3P}(\tilde{\gamma}',\gamma_1,\gamma_2,\mathbf{q}=0,\mathbf{k})\\
&\times\frac{\left(\gamma'-\frac{1}{2}\right)^2}{\gamma'^2(1-\gamma')^2}{\rm e}^{\omega(\gamma')Y_2}E(\mathbf{p}_2,\mathbf{q},n=0,\tilde{\gamma}')\,.
\end{aligned}\tag{38}$$

Recall that the definition of the conformal variable γ is $\gamma=(n+1)/2+{\rm i}\nu$, and for the largest contribution one takes the $n=0$ contribution only, for high energies, such that $\gamma=1/2+{\rm i}\nu$. Hence, in terms of the variables ν, ν', ν_1 and ν_2, the limits of integration are $+\infty-{\rm i}\epsilon\geq\nu\geq-\infty-{\rm i}\epsilon$, and similarly one has the same integration limits for the integrals over ν', ν_1 and ν_2. In each case one takes the limit that ϵ tends to zero. Hence, in terms of these variables, the expression of (38) can be recast in the following form:

$$\begin{aligned}
&P^{\rm BFKL}_{\rm enhanced}(\mathbf{p}_1,\mathbf{p}_2,Y,\mathbf{q})=B\int_{-\infty}^{\infty}{\rm d}\nu\int_{-\infty}^{\infty}{\rm d}\nu'\int_{-\infty}^{\infty}{\rm d}\nu_1\\
&\times\int_{-\infty}^{\infty}{\rm d}\nu_2\int{\rm d}^2k\int_{Y_{\rm H}+\frac{1}{2}\delta Y_{\rm H}}^{Y}{\rm d}Y_1\int_0^{Y_{\rm H}-\frac{1}{2}\delta Y_{\rm H}}{\rm d}Y_2\\
&\times E(\mathbf{p}_1,\mathbf{q},\nu)\mathcal{D}(\nu){\rm e}^{\omega(\nu)(Y-Y_1)}G_{3P}(\nu,\nu_1,\nu_2,\mathbf{q}=0,\mathbf{k})\\
&\times\mathcal{D}(\nu_1)\mathcal{D}(\nu_2){\rm e}^{(\omega(\nu_1)+\omega(\nu_2))(Y_1-Y_2)-\omega(\nu_2)\delta Y_{\rm H}}\\
&\times G_{3P}(-\nu',\nu_1,\nu_2,\mathbf{q}=0,\mathbf{k}){\rm e}^{\omega(\nu')Y_2}E(\mathbf{p}_2,\mathbf{q},-\nu')\,,
\end{aligned}\tag{39}$$

where $Y_{\rm H}$ is the rapidity of the Higgs boson. $Y_{\rm H}$ here is considered to be equal to zero in the c.m. frame, restricting ourselves to the production of the Higgs boson at rest in the center of mass frame since it is the most likely experimental kinematics, and $\delta Y_{\rm H}=\ln\left(M_H^2/4m^2\right)$ characterizes the rapidity window occupied by the Higgs boson. Using the same assumptions as Sect. 2.2, the integral over $\mathbf{k}$ in (39) is evaluated in the appendix with the result given in (A.18) as

$$\begin{aligned}
&\int{\rm d}^2kG_{3P}(\nu,\nu_1\to0,\nu_2\to0,\mathbf{q}=0,\mathbf{k})\\
&\times G_{3P}(-\nu',\nu_1\to0,\nu_2\to0,\mathbf{q}=0,\mathbf{k})\\
&\xrightarrow{\nu_1,\nu_2\to0}\frac{2^{2({\rm i}\nu'-{\rm i}\nu)}}{8}\frac{\delta(\nu-\nu')}{4\nu_1^2 4\nu_2^2}\\
&\times\frac{\Gamma^3\left(\frac{1}{2}+{\rm i}\nu'\right)\Gamma^3\left(\frac{1}{2}-{\rm i}\nu\right)\Gamma^2(-{\rm i}\nu')\Gamma^2({\rm i}\nu)}{\Gamma\left(\frac{1}{2}-{\rm i}\nu'\right)\Gamma\left(\frac{1}{2}+{\rm i}\nu\right)}\,.
\end{aligned}\tag{40}$$

Note that ν_1^2 and ν_2^2 in the denominator of (40) cancel with $\mathcal{D}(\nu_1)$ and $\mathcal{D}(\nu_2)$ in (39) (see (28)). When inserting (40) into the right hand side of (39), the delta function is absorbed in the integration over ν', to give the result

$$\begin{aligned}
&P^{\rm BFKL}_{\rm enhanced}(\mathbf{p}_1,\mathbf{p}_2,Y,\mathbf{q}=0)=\frac{B\pi^2}{8}\int_{-\infty}^{\infty}{\rm d}\nu\int_{-\infty}^{\infty}{\rm d}\nu_1\\
&\int_{-\infty}^{\infty}{\rm d}\nu_2\int_{Y_{\rm H}+\frac{1}{2}\delta Y_{\rm H}}^{Y}{\rm d}Y_1\int_0^{Y_{\rm H}-\frac{1}{2}\delta Y_{\rm H}}{\rm d}Y_2
\end{aligned}$$

$$\times E(\mathbf{p}_1,\mathbf{q},\nu)\mathcal{D}^2(\nu)\mathrm{e}^{\omega(\nu)(Y-Y_1+Y_2)}\frac{\Gamma^2\left(\frac{1}{2}-\mathrm{i}\nu\right)\Gamma^2\left(\frac{1}{2}+\mathrm{i}\nu\right)}{4\nu_1^2 4\nu_2^2\nu^2\sin^2(\mathrm{i}\nu\pi)}$$
$$\times\mathcal{D}(\nu_1)\mathcal{D}(\nu_2)\mathrm{e}^{(\omega(\nu_1)+\omega(\nu_2))(Y_1-Y_2)-\omega(\nu_2)\delta Y_{\mathrm{H}}}E(\mathbf{p}_2,\mathbf{q},-\nu)\,. \tag{41}$$

Now the integrals over ν,ν_1,ν_2 and the two rapidity values Y_1 and Y_2 need to be evaluated. Y_1 and Y_2 are the upper and lower rapidity values for the pomeron loop in Fig. 7. The details of the integrations are given in Sect. A.2 of the appendix, and the final expression is given in (A.51) as

$$P^{\mathrm{BFKL}}_{\mathrm{enhanced}}(\mathbf{p}_1,\mathbf{p}_2,Y,\mathbf{q}=0)=\frac{32B\pi^8}{(2\bar{\alpha}_{\mathrm{s}})^5p^2}$$
$$\times\frac{\delta Y_{\mathrm{H}}}{\omega''(\nu=0)Y^{1/2}(Y-\delta Y_{\mathrm{H}})^{1/2}}$$
$$\times\left((2\omega(\nu=0))^4-2\frac{(2\omega''(\nu=0))^3}{Y}-2\frac{(2\omega''(\nu=0))^3}{Y-\delta Y_{\mathrm{H}}}\right)$$
$$\times\mathrm{e}^{2\omega(\nu=0)\left(Y-\frac{1}{2}\delta Y_{\mathrm{H}}\right)}\,, \tag{42}$$

where the constant B is given in (36). Therefore, the full expression for the diagram of Fig. 7 given by (34) takes the form

$$M_{\mathrm{Higgs}}(n=2,Y)=\frac{64B\pi^8}{(2\bar{\alpha}_{\mathrm{s}})^5p^2}$$
$$\times\frac{\delta Y_{\mathrm{H}}}{\omega''(\nu=0)Y^{1/2}(Y-\delta Y_{\mathrm{H}})^{1/2}}$$
$$\times\left((2\omega(\nu=0))^4-2\frac{(2\omega''(\nu=0))^3}{Y}-2\frac{(2\omega''(\nu=0))^3}{Y-\delta Y_{\mathrm{H}}}\right)$$
$$\times\mathrm{e}^{2\omega(\nu=0)\left(Y-\frac{1}{2}\delta Y_{\mathrm{H}}\right)}A_{\mathrm{H}}(\delta Y_{\mathrm{H}})\,. \tag{43}$$

3 The survival probability in diffractive Higgs production in color dipole scattering due to pomeron exchange

3.1 The definition of survival probability

In this section the survival probability of large rapidity gaps, in diffractive Higgs production, is calculated, using the ratio of Figs. 4 and 7 (see (31) and (43)). To guarantee that there will still be a large rapidity gap (LRG) between the protons after scattering, all hard rescattering corrections that could give terms filling up the LRG must be taken into account. The survival probability is the probability to just have exclusive Higgs production shown in Fig. 4, and not any higher order hard rescattering corrections, such as the first enhanced diagram of Fig. 7. In other words, the survival probability of the LRG is calculated by subtracting the sum over all hard rescattering amplitudes from the single pomeron amplitude of Fig. 4, dividing the result by the single pomeron amplitude of Fig. 4 itself, to obtain the correctly normalized survival probability. Therefore, the survival probability is defined by

$$\langle|S^2|\rangle=\frac{M_{\mathrm{Higgs}}(n=1,Y)-\sum_{n=2}^{\infty}(-1)^nM_{\mathrm{Higgs}}(n,Y)}{M_{\mathrm{Higgs}}(n=1,Y)}\,, \tag{44}$$

where $M_{\mathrm{Higgs}}(n,Y)$ is the nth order hard rescattering correction. For example, in the case of $n=2$, the first hard rescattering correction $M_{\mathrm{Higgs}}(n=2,Y)$ is the contribution of the first enhanced diagram of Fig. 7, which has two pomeron branches, forming the pomeron loop. In general, $M_{\mathrm{Higgs}}(n,Y)$ is the contribution given by the diagram which has n pomeron branches. In calculating the survival probability, if only the first enhanced diagram is taken into account, and corrections of the order $n=3$ and higher are ignored, then (44) reduces to

$$\langle|S^2|\rangle=\frac{M_{\mathrm{Higgs}}(n=1,Y)-M_{\mathrm{Higgs}}(n=2,Y)}{M_{\mathrm{Higgs}}(n=1,Y)}$$
$$=1-\frac{M_{\mathrm{Higgs}}(n=2,Y)}{M_{\mathrm{Higgs}}(n=1,Y)}\,. \tag{45}$$

The ratio $\frac{M_{\mathrm{Higgs}}(n=2,Y)}{M_{\mathrm{Higgs}}(n=1,Y)}$ is calculated in the next subsection, in the symmetric QCD dipole approach (see (49) in Sect. 3.2). It turns out that this ratio is not small and, therefore, all enhanced diagrams need to be taken into account. Using the toy model suggested by Mueller in [6], all enhanced diagrams are taken into account in the Mueller–Patel–Salam–Iancu (MPSI) approach [23–25]. The formula for the scattering amplitude in this model was suggested by Kovchegov in [26].

3.2 The QCD dipole approach

The survival probability of large rapidity gaps, in diffractive Higgs production in the QCD dipole approach, is the probability for the exclusive Higgs production of Fig. 4, with a large rapidity gap between the Higgs signal and the two emerging dipoles. To calculate the survival probability, all hard rescattering corrections which could fill up the large rapidity gaps must be subtracted from the single BFKL Higgs amplitude $M_{\mathrm{Higgs}}(n=1,Y)$, and the result must be divided by $M_{\mathrm{Higgs}}(n=1,Y)$. If only the first enhanced rescattering correction $M_{\mathrm{Higgs}}(n=2,Y)$ is taken into account, then the survival probability in the symmetric QCD dipole approach is estimated to be

$$\langle|S^2|\rangle=\frac{M_{\mathrm{Higgs}}(n=1,Y)-M_{\mathrm{Higgs}}(n=2,Y)}{M_{\mathrm{Higgs}}(n=1,Y)}$$
$$=1-\frac{M_{\mathrm{Higgs}}(n=2,Y)}{M_{\mathrm{Higgs}}(n=1,Y)}\,, \tag{46}$$

where the amplitudes $M(n=1,Y)$ and $M(n=2,Y)$ have been calculated in (31) and (43), respectively. Using the results of (31) and (43), the ration $\frac{M(n=2,Y)}{M(n=1,Y)}$ appearing

in (46) is found to obey the expression

$$\frac{M_{\text{Higgs}}(n=2,Y)}{M_{\text{Higgs}}(n=1,Y)} = \frac{2B\pi^5}{\alpha_{\text{s}}^2(2\bar{\alpha}_{\text{s}})^5}\frac{\delta Y_{\text{H}}}{\omega''(\nu=0)} \times \left(\frac{(2\omega(\nu=0))^4}{Y} - 4\frac{(2\omega(\nu=0))^3}{Y^2}\right)\left(\frac{\omega''(\nu=0)Y}{2\pi}\right)^{\frac{1}{2}} \times \mathrm{e}^{\omega(\nu=0)Y}\,, \tag{47}$$

where the constant B is given in (36). Here a typical value for α_{s}, at the scale of M_Z, the mass of the Z boson, is used. It is expected that the Higgs boson will be produced with a mass of approximately 100 GeV, which would give a value for the strong coupling constant $\alpha_{\text{s}} \sim 0.12$. This corresponds to a Z particle mass [27] $M_Z = 90.8 \pm 0.6$ GeV.

The following values are to be found in [27, 28] for the strong coupling and the BFKL function:

$$\alpha_{\text{s}} = 0.12\,, \quad \omega(\nu=0) = \bar{\alpha}_{\text{s}} 4\ln 2\,, \quad \frac{1}{2}\omega''(\nu=0) = 14\bar{\alpha}_{\text{s}}\,, \quad \zeta(3)\zeta(3) \cong 1.202\,. \tag{48}$$

Assuming that the rapidity gap Y at the LHC is 19, and using the numerical values given in (48), the right hand side of (47) yields following:

$$\frac{M(n=2,Y)}{M(n=1,Y)} = 2.8\mathrm{e}^{\omega(\nu=0)Y}\,. \tag{49}$$

This value is not small and increases with energy. Therefore, it shows that all enhanced diagrams have to be taken into account. In the next section all enhanced diagrams are summed in the toy model.

3.3 The toy model approach

In this subsection, the survival probability is calculated taking into account all enhanced diagrams. The toy model proposed by Mueller in [6], is a model for describing pomeron exchange in onium–onium scattering. In the toy model, the dipole wave function of an onium is described by the generating functional for dipoles [6] $Z(Y,[u])$:

$$Z(Y-Y_0;[u]) \equiv \sum_{n=1}\int P_n(Y;r_1,b_1,r_2,b_2,\ldots,r_i,b_i,\ldots,r_n,b_n) \times \prod_{i=1}^{n} u(r_i,b_i)\,\mathrm{d}^2r_i\,\mathrm{d}^2b_i\,. \tag{50}$$

Here, P_n are the probabilities to find dipoles with sizes r_i and impact parameters b_i at rapidity Y, and $u(x_{01},b)$ is an arbitrary function of the dipole of transverse size x_{01} at impact parameter b. In the toy model which we are going to consider here we neglect the dependence of u on the size of dipoles and their impact parameters [6]. In this model $Z(x_{01},b,Y,u)$ degenerates to the generating function and obeys the following evolution equation [6]:

$$\frac{\mathrm{d}Z(Y,u)}{\mathrm{d}Y} = \Delta Z^2(Y,u) - \Delta Z(Y,u)\,, \tag{51}$$

where Δ is the pomeron intercept. In Sects. 2.3 and 2.4, the pomeron intercept can be taken to be the BFKL intercept $\Delta = \omega(\nu=0)$ to provide a matching with the BFKL pomeron calculus. The initial condition for (51) is given by

$$Z(Y=0,u) = u\,. \tag{52}$$

The solution of the toy model (51) which satisfies the initial condition of (52) is [6, 26]

$$Z(Y,u) = \frac{u}{u+(1-u)\mathrm{e}^{\Delta Y}}\,. \tag{53}$$

Equation (53) gives the sum over all "fan" diagrams. To generalize this result to the sum over all essential enhanced diagrams, the MPSI approximation is used to sum over all diagrams, with pomeron loops larger than $\frac{Y}{2}$. In [26], the forward scattering amplitude in the MPSI approximation was written, and it has the form

$$D(Y,d) = 1 - \exp\left(-d\frac{\mathrm{d}^2}{\mathrm{d}u\,\mathrm{d}v}\right) Z\left(\frac{Y}{2},u\right) \times Z\left(\frac{Y}{2},v\right)|_{u=1,v=1}\,, \tag{54}$$

where d is the dipole amplitude ($0 < d < 1$) at low energy. Substituting for $Z(Y,u)$, the right hand side of (53) in (54) yields the following expression for $D(Y,d)$ [26]:

$$D(Y,d) = -\sum_{n=1}^{\infty}(-1)^n D(n,Y,d) = -\sum_{n=1}^{\infty} n!(-1)^n d^n \mathrm{e}^{n\Delta Y}\left(1-\mathrm{e}^{\Delta\frac{Y}{2}}\right)^{2n-2}\,. \tag{55}$$

At large rapidity values, one can make the approximation $1-\mathrm{e}^{\Delta\frac{Y}{2}} \approx -\mathrm{e}^{\Delta\frac{Y}{2}}$, so that (55) can be rewritten as

$$D(Y,d) = -\sum_{n=1}^{\infty}(-1)^n D(n,Y,d) = -\sum_{n=1}^{\infty} n!(-1)^n d^n \mathrm{e}^{n\Delta Y}\,. \tag{56}$$

In (56), the nth term is the amplitude for n pomeron exchange. Hence, (56) is the sum over all hard rescattering correction amplitudes for pomeron exchange in onium–onium scattering. This approach is used in [23–25]. To include Higgs production in the toy model, one has to replace one of the n dipole amplitudes by the contribution $A_{\text{H}}(\delta Y_{\text{H}})$ from the subprocess for Higgs production. The leading subprocess is the quark triangle shown in Fig. 6. Hence, for each of the terms, a factor of n is included to account for the possibility that the Higgs boson can be produced from any of the n pomerons. After Higgs production is included in the toy model of (56), the resulting amplitude

takes the form

$$\begin{aligned} D_{\rm Higgs}(Y,d) &= -\sum_{n=1}^{\infty}(-1)^n D_{\rm Higgs}(n,Y,d) \\ &= -\sum_{n=1}^{\infty}(-1)^n d^{n-1} n! n \mathrm{e}^{n\Delta Y} A_{\rm H}(\delta Y_{\rm H}) \\ &= \frac{\partial}{\partial d} D(Y,d) A_{\rm H}(\delta Y_{\rm H})\,, \end{aligned} \tag{57}$$

where

$$\begin{aligned} D_{\rm Higgs}(n,Y,d) &= d^{n-1} n! n \mathrm{e}^{n\Delta Y} A_{\rm H}(\delta Y_{\rm H}) \\ &= \frac{\partial}{\partial d} D(n,Y,d) A_{\rm H}(\delta Y_{\rm H})\,. \end{aligned} \tag{58}$$

The notation $D_{\rm Higgs}(n,Y,d)$ refers to the toy model BFKL pomeron amplitude, including Higgs production, with n pomeron branches. This should not be confused with the notation $M_{\rm Higgs}(n,Y)$, which refers to the equivalent nth order term in the symmetric QCD dipole approach. The $n=1$ term in (57), corresponds to the single pomeron amplitude of Fig. 4. The $n=2$ term in (57) corresponds to the first enhanced amplitude of Fig. 7, with the hard rescattering correction of the pomeron loop. In Sect. 3.1, the survival probability was defined by the expression given in (44). Hence, in the toy model approach, the survival probability takes the form

$$\frac{D_{\rm Higgs}(n=1,Y,d) - \sum_{n=2}^{\infty}(-1)^n D_{\rm Higgs}(n,Y,d)}{D_{\rm Higgs}(n=1,Y,d)}\,. \tag{59}$$

Inspection of (57) shows that the numerator on the RHS of (59) can be rewritten as

$$\begin{aligned} &D_{\rm Higgs}(Y,d) = \\ &D_{\rm Higgs}(n=1,Y,d) - \sum_{n=2}^{\infty}(-1)^n D_{\rm Higgs}(n,Y,d)\,. \end{aligned} \tag{60}$$

Hence, the toy model formula for the survival probability of (59) becomes

$$\frac{D_{\rm Higgs}(Y,d)}{D_{\rm Higgs}(n=1,Y,d)} = \frac{\frac{\partial}{\partial d} D(Y,d)}{\frac{\partial}{\partial d} D(n=1,Y,d)}\,. \tag{61}$$

Typically, the Higgs signal will occupy a rapidity window $\delta Y_{\rm H} = \ln \frac{M_H^2}{4m^2}$. Therefore, in the toy model, pomeron exchange between scattering dipoles separated by a rapidity gap of less than $\delta Y_{\rm H}$ should be excluded for Higgs production. Therefore, the toy model amplitude $M_{\rm Higgs}(n,Y,d)$ should be divided by the scattering amplitude $M_{\rm Higgs}(n, \delta Y_{\rm H}, d)$, which gives the scattering amplitude for dipoles separated by a rapidity gap less than $\delta Y_{\rm H}$. Taking this into account, (61) is modified to give the survival probability for diffractive Higgs production within the rapidity window $\delta Y_{\rm H}$:

$$\langle |S^2| \rangle = \frac{\left(\frac{\partial}{\partial d} D(Y,d)\right) / \left(\frac{\partial}{\partial d} D(\delta Y_{\rm H},d)\right)}{\left(\frac{\partial}{\partial d} D(n=1,Y,d)\right) / \left(\frac{\partial}{\partial d} D(n=1,\delta Y_{\rm H},d)\right)}\,. \tag{62}$$

In order to calculate the survival probability using the expression of (59), the value of the parameter d, appearing in the expression for $D(Y,d)$, must be determined. To do so, it is useful to refer back to the calculation of Sect. 3.2, where the ratio $\frac{M_{\rm Higgs}(n=2,Y)}{M_{\rm Higgs}(n=1,Y)}$ was calculated, in the symmetric QCD dipole approach (see (49)). In order for the toy model to be consistent with the QCD dipole approach, the ratio calculated in (49) should be the same in the toy model. Setting $n=1$, (58) gives for single pomeron amplitude in the toy model

$$D_{\rm Higgs}(n=1,Y,d) = \mathrm{e}^{\Delta Y} A_{\rm H}(\delta Y_{\rm H})\,. \tag{63}$$

Setting $n=2$ in (58), the first enhanced amplitude in the toy model is given by

$$D_{\rm Higgs}(n=2,Y,d) = -4d\mathrm{e}^{2\Delta Y} A_{\rm H}(\delta Y_{\rm H})\,. \tag{64}$$

Therefore, using (63) and (64), the following condition is imposed:

$$\begin{aligned} \frac{M_{\rm Higgs}(n=2,Y)}{M_{\rm Higgs}(n=1,Y)} &= \frac{D_{\rm Higgs}(n=2,Y,d)}{D_{\rm Higgs}(n=1,Y,d)} \\ &= \frac{-4d^2\mathrm{e}^{2\Delta Y} A_{\rm H}(\delta Y_{\rm H})}{d\mathrm{e}^{\Delta Y} A_{\rm H}(\delta Y_{\rm H})} = -4d\mathrm{e}^{\Delta Y}\,. \end{aligned} \tag{65}$$

Substituting for $\frac{M_{\rm Higgs}(n=2,Y)}{M_{\rm Higgs}(n=1,Y)}$ the result of (49) on the LHS of (65), and setting the pomeron intercept equal to the BFKL intercept $\Delta = \omega(\nu=0)$, to be consistent with the QCD dipole approach, enables one to calculate a value for d in the toy model. One finds

$$d = 0.7\,. \tag{66}$$

One can now proceed to calculate the survival probability, by taking into account all higher additional hard rescattering corrections, using the formula of (61). From (56), the expression for $D(Y,d)$ can be written as

$$\begin{aligned} D(Y,d) &= -\sum_{n=1}^{\infty} n!(-d\mathrm{e}^{\Delta Y})^n \\ &= -\sum_{n=1}^{\infty}\int_0^{\infty} \mathrm{d}t \mathrm{e}^{-t}(-\mathrm{d}t\mathrm{e}^{\Delta Y})^n \\ &= 1 - \int_0^{\infty} \mathrm{d}t \frac{\mathrm{e}^{-t}}{1+\mathrm{d}t\mathrm{e}^{\Delta Y}}\,. \end{aligned} \tag{67}$$

After changing variables to $u = \frac{1}{d\mathrm{e}^{\Delta Y}} + t$, the RHS reduces to

$$\begin{aligned} D(Y,d) &= 1 - \frac{\exp\left(\frac{1}{d\mathrm{e}^{\Delta Y}}\right)}{d\mathrm{e}^{\Delta Y}} \int_{\frac{1}{d\mathrm{e}^{\Delta Y}}}^{\infty} \frac{du\mathrm{e}^{-u}}{u} \\ &= 1 - \frac{\exp\left(\frac{1}{d\mathrm{e}^{\Delta Y}}\right)}{d\mathrm{e}^{\Delta Y}} \Gamma\left(0, \frac{1}{d\mathrm{e}^{\Delta Y}}\right)\,. \end{aligned} \tag{68}$$

If one notes that in general $\frac{\mathrm{d}}{\mathrm{d}x}\Gamma(0,x) = -\frac{\mathrm{e}^{-x}}{x}$, then substituting for $D(Y,d)$ the RHS of (68) in (62) gives the following expression for the survival probability:

$$\langle|S^2|\rangle = \left(\frac{\mathrm{e}^{2\Delta\delta Y_{\mathrm{H}}}}{\mathrm{e}^{2\Delta Y}}\right) \times \left(\frac{\exp\left(\frac{1}{d\mathrm{e}^{\Delta Y}}\right)\Gamma\left(0,\frac{1}{d\mathrm{e}^{\Delta Y}}\right)\left(\frac{1+d\mathrm{e}^{\Delta Y}}{d\mathrm{e}^{\Delta Y}}\right) - d}{\exp\left(\frac{1}{d\mathrm{e}^{\Delta\delta Y_{\mathrm{H}}}}\right)\Gamma\left(0,\frac{1}{d\mathrm{e}^{\Delta\delta Y_{\mathrm{H}}}}\right)\left(\frac{1+d\mathrm{e}^{\Delta\delta Y_{\mathrm{H}}}}{d\mathrm{e}^{\Delta\delta Y_{\mathrm{H}}}}\right) - d}\right). \quad (69)$$

The typical rapidity window δY_{H}, which the Higgs signal is expected to occupy, is $\delta Y_{\mathrm{H}} = \ln\left(\frac{M_H^2}{4m^2}\right)$, where $M_H^2 \sim 100\,\mathrm{GeV}$. The typical rapidity gap is expected to be $Y = 19$ for the LHC energy of $\sqrt{s} = 14\,\mathrm{TeV}$. Setting the pomeron intercept equal to the BFKL intercept, $\Delta_{\mathrm{BFKL}} = \omega(\nu = 0) = \bar{\alpha}_{\mathrm{s}} 4\ln 2 \approx 0.34$ [28], the value for the survival probability from (69) is found to be

$$\langle|S^2(\Delta_{\mathrm{BFKL}})|\rangle = 0.004\,. \quad (70)$$

This gives the survival probability as 0.4%. However, the larger survival probability is obtained by abandoning the BFKL intercept $\omega(\nu = 0) \approx 0.34$ and replacing the intercept with that of the intercept of the soft pomeron. The intercept of the soft pomeron is intended to mean the phenomenological intercept of the Landshoff–Donachie pomeron. This intercept (denoted here as Δ_{soft}) is proportional to the strong coupling α_{s} by the relation $\Delta_{\mathrm{soft}} = c\alpha_{\mathrm{s}} = 0.08$. Hence, if one takes the strong coupling to be $\alpha_{\mathrm{s}} = 0.12$ for example, then the constant of proportionality $c = 0.067$. In this case, using Δ_{soft} as the pomeron intercept in (69), one obtains the following value for the survival probability:

$$\langle|S^2(\Delta_{\mathrm{soft}})|\rangle = 0.3\,. \quad (71)$$

More recently the Durham group found [31] the value for the soft pomeron intercept to be $\Delta_{\mathrm{Durham\ group}} = 0.6$, which gives for the survival probability

$$\langle|S^2(\Delta_{\mathrm{Durham\ group}})|\rangle = 5\times10^{-6}\,. \quad (72)$$

The values found for the survival probability, which depends on the choice of intercept, are summarized in Table 1.

Therefore, from these results it is clear that the survival probability depends critically on the intercept chosen. More specifically, the survival probability, as a function of the intercept Δ is not monotonic. The survival probability increases, as the intercept Δ decreases in value. For large rapidity gaps Y, from (69), the survival probability is approximately proportional to

$$\langle|S^2(\Delta)|\rangle \propto \frac{1}{\exp(2\Delta(Y-\delta Y_{\mathrm{H}}))}\,. \quad (73)$$

The typical LHC value for the rapidity gap Y between the scattering dipoles is $Y = 19$, and for the predicted Higgs mass of M_H^2, the rapidity window occupied by the Higgs boson, is expected to be $\delta Y_{\mathrm{H}} = \ln\left(\frac{M_H^2}{4m^2}\right)$. Hence, provided that $Y - \delta Y_{\mathrm{H}} > 0$, (73) explains why the survival probability increases as the intercept Δ decreases.

pomeron intercept	survival probability
$\Delta_{\mathrm{Durham\ group}}$	5×10^{-6}
Δ_{BFKL}	0.004
Δ_{soft}	0.3

Table 1. Results for the survival probability for different Pomeron intercepts

Based on these results, in the toy model, the hard rescattering contributions from higher n corrections range from 0.4% up to around 10%. Hence, the corrections are substantial and need to be taken into account when calculating the survival probability. d in the toy model takes the value found in (66) to be $d = 0.7$. This is less than unity. By inspection of the summation in (57), one can see that d is large enough, so that the terms $n = 3$ and higher will give significant corrections to the survival probability calculated in this paper.

To summarize, it is found, firstly, that d is large, giving significant higher contributions. Secondly, these higher contributions need to be taken into account, when calculating the survival probability.

4 Conclusion

The main results of this paper are the following.

1. The first calculation of the enhanced BFKL diagram for diffractive Higgs production.
2. Estimates for the survival probability for the full set of enhanced diagrams using the simplified toy model.
3. The results of this estimate for the survival probability, show that the value depends crucially on the coupling constant of QCD, and that multi-pomeron exchange gives a substantial contribution to the survival probability.

It was found that in the most consistent result for the survival probability, the value is rather small, namely 0.4%. In conclusion, this paper shows that hard processes give a substantial contribution in the calculation of the survival probability. This paper is the first step forward towards obtaining reliable estimates of the influences of hard processes at high energy.

Acknowledgements. This paper is dedicated to my Mum and Dad. I would like to thank E. Gotsman, A. Kormilitzin, E. Levin and A. Prygarin for fruitful discussions on the subject. This research was supported in part by the Israel Science Foundation, founded by the Israeli Academy of Science and Humanities, by a grant from the Israeli ministry of science, culture & sport, and the Russian Foundation for Basic research of the Russian Federation, and by the BSF Grant No. 20004019.

Appendix

A.1 Calculation of the triple pomeron vertex

In this section the triple pomeron vertex is calculated to give an explicit expression in the momentum representation. This will be useful for calculating the first enhanced diagram of Fig. 7 in Sect. 2.4. In the expression for Fig. 7, (see (39)), the BFKL functions $\omega(\nu_1)$ and $\omega(\nu_2)$ are expanded around the saddle points $\nu_1 = \nu_2 = 0$. This gives the largest contribution to the integration. Hence, in this subsection the triple pomeron vertex is calculated in the limiting case when $\nu_1 = \nu_2 = 0$. It is assumed at the start of the calculation that ν_1 and ν_2 are small and finite; however, at the end of the calculation ν_1 and ν_2 are put equal to zero. The triple pomeron vertex shown in Fig. 3 was defined in Sect. 2.2 (see (19)). We have

$$G_{3P}(\mathbf{q},\mathbf{k},n=0,\gamma,\gamma_1,\gamma_2) = G_{3P}(\mathbf{q},\mathbf{k},\nu,\nu_1,\nu_2) = \int \frac{\mathrm{d}^2x_{10}\,\mathrm{d}^2x_{20}\,\mathrm{d}^2x_{30}}{x_{12}x_{23}x_{31}} E_q^{n,\nu}(x_{10},x_{20}) E_k^{n,\nu_1}(x_{20},x_{30}) \times E_{q-k}^{n,\nu_2}(x_{30},x_{10})\,. \tag{A.1}$$

A useful expression, to be found in [13], was given in (20) in terms of the mixed representation of the vertex function $E_k^{n,\nu}(\mathbf{x})$ (see (8)) as

$$G_{3P}(\mathbf{q}=0,\mathbf{k},\nu,\nu_1,\nu_2) = \frac{1}{2\pi}\int \frac{\mathrm{d}^2x_{01}}{x_{01}^2} x_{01}^{-2\mathrm{i}\nu-1} \mathrm{e}^{\frac{\mathrm{i}\mathbf{k}\cdot\mathbf{x}_{01}}{2}} \times \int \mathrm{d}^2x_2 \frac{x_{01}^2}{x_{12}^2x_{02}^2} x_{02}^{2\mathrm{i}\nu_1+1} E_k^{n,\nu_1}(x_{02}) x_{12}^{2\mathrm{i}\nu_2+1} E_{-k}^{n,\nu_2}(x_{12})\,. \tag{A.2}$$

In (A.2), it is assumed that $\mathbf{q}$ in Fig. 3 is zero. This is because for the calculation of the first enhanced diagram in Sect. 2.4 (see Fig. 7), the momentum $\mathbf{q}$ transferred along the pomeron above and below the loop is set to zero to make the calculation simpler. In Fig. 7, there are two triple pomeron vertices, at opposite ends of the pomeron loop. Here, the momentum $\mathbf{k}$ is the unknown momentum in the pomeron loop. Evaluating the integral over x_{01} in (A.2) gives an expression in which the dependence on the momentum $\mathbf{k}$ is explicit, namely [13]

$$G_{3P}(\mathbf{q}=0,\mathbf{k},\nu,\nu_1,\nu_2) = 2^{3-2\gamma-2\gamma_1-2\gamma_2}(k^2)^{\mathrm{i}\nu+\mathrm{i}\nu_1+\mathrm{i}\nu_2-\frac{1}{2}} \times \frac{\Gamma\left(\frac{1}{2}-\mathrm{i}\nu-\mathrm{i}\nu_1-\mathrm{i}\nu_2\right)}{\Gamma\left(\frac{1}{2}+\mathrm{i}\nu+\mathrm{i}\nu_1+\mathrm{i}\nu_2\right)} g_{3P}(\gamma,\gamma_1,\gamma_2)\,, \tag{A.3}$$

where $g_{3P}(\gamma,\gamma_1,\gamma_2)$ is the multidimensional integral related to the triple BFKL pomeron interaction, given by [13]

$$g_{3P}(\gamma,\gamma_1,\gamma_2) = \int \frac{\mathrm{d}^2x}{|x_+|^{2-2\gamma_1}|x_-|^{2-2\gamma_2}} \int \frac{\mathrm{d}^2R}{|R_+|^{2\gamma_1}|R_-|^{2\gamma_1}} \times \int \frac{\mathrm{d}^2R'}{|R'_+|^{2\gamma_2}|R'_-|^{2\gamma_2}} |R_- - R'_-|^{2\gamma+2\gamma_1+2\gamma_2-4}, \tag{A.4}$$

where in the notation of [13],

$$\begin{aligned} &\gamma = \frac{1}{2}+\mathrm{i}\nu\,, && \gamma_1 = \frac{1}{2}+\mathrm{i}\nu_1\,, && \gamma_2 = \frac{1}{2}+\mathrm{i}\nu_2\,,\\ &x_+ = x+\frac{n}{2}\,, && x_- = x-\frac{n}{2}\,, && R_+ = R+\frac{x_+}{2}\,,\\ &R_- = R-\frac{x_+}{2}\,, && R'_+ = R'+\frac{x_-}{2}\,, && R'_- = R'-\frac{x_-}{2}\,. \end{aligned} \tag{A.5}$$

The region of integration in (41) that turns out to give the largest contribution is the region close to $\mathrm{i}\nu \to \frac{1}{2}$, and the region close to $|\nu_1| \to 0$ and $|\nu_2| \to 0$. A complete argument for this claim is given in Sect. A.2 of the appendix, for the reason that this region gives a vanishing contribution to the first enhanced amplitude, when it comes to integrating over the two rapidity variables Y_1 and Y_2 (see (39)). For now it will be assumed in the derivation of the relevant expression of the triple pomeron vertex that the region close to $|\nu_1| \to 0$ and $|\nu_2| \to 0$ is the only relevant region necessary to consider. With this in mind, with the definition in (A.5), the relevant region of integration is close to the points where

$$\gamma \to 1 \gamma_1 \to \frac{1}{2}\gamma_2 \to \frac{1}{2} \Rightarrow \gamma+\gamma_1+\gamma_2 \to 2\,. \tag{A.6}$$

Consider the part of the integration over R' in (A.4), which takes the form

$$\int \frac{\mathrm{d}^2R'}{\left(R'_+\right)^{2\gamma_2}\left(R'_-\right)^{2\gamma_2}} \left(R_- - R'_-\right)^{2\gamma+2\gamma_1+2\gamma_2-4} = \int \frac{\mathrm{d}R'}{\left(R'_+\right)^{\gamma_2}\left(R'_-\right)^{\gamma_2}} \left(R_- - R'_-\right)^{\gamma+\gamma_1+\gamma_2-2} \times \int \frac{\mathrm{d}R'^*}{\left(R'^*_+\right)^{\gamma_2}\left(R'^*_-\right)^{\gamma_2}} \left(R^*_- - R'^*_-\right)^{\gamma+\gamma_1+\gamma_2-2}\,. \tag{A.7}$$

In (A.7) the complex notation $\mathrm{d}^2R' = \mathrm{d}R'\,\mathrm{d}R'^*$ has been used. Evaluating the integrations over R' and R'^* gives

$$\begin{aligned} &\int \frac{\mathrm{d}R'}{\left(R'_+\right)^{\gamma_2}\left(R'_-\right)^{\gamma_2}} \left(R_- - R'_-\right)^{\gamma+\gamma_1+\gamma_2-2} = \\ &\pi^{\frac{1}{2}} \frac{\Gamma\left(\frac{3}{2}-\gamma_1-\gamma_2-\gamma\right)}{\Gamma\left(2-\gamma-\gamma_1-\gamma_2\right)} \frac{\left(R_+-(x_+-x)\right)^{\gamma_1+\gamma_2+\gamma-\frac{3}{2}}}{x_-^{\frac{1}{2}}} {}_2F_1 \\ &\times \left(\frac{1}{2},\frac{1}{2},\gamma_1+\gamma_2+\gamma-\frac{1}{2},\frac{R_+-(x_+-x)}{x_-}\right) \\ &+\pi^{-\frac{1}{2}}\Gamma\left(2-\gamma-\gamma_1-\gamma_2\right)\Gamma\left(\gamma+\gamma_1+\gamma_2-\frac{3}{2}\right) \\ &\times x_-^{(\gamma+\gamma_1+\gamma_2)-2}\,. \end{aligned} \tag{A.8}$$

Inspection of the right hand side of (A.8) shows that one has a singularity at $\gamma+\gamma_1+\gamma_2 \to 2$, which is the point defined in (A.6), namely focussing on the case when $\mathrm{i}\nu \to \frac{1}{2}$ and $|\nu_1| = |\nu_2| = 0$ (see (A.5)). In this case, $\Gamma(2-\gamma-\gamma_1-\gamma_2)$ tends to infinity, which means that the first term on the RHS of (A.8) vanishes and the second term gives the

largest contribution. There is one more singularity present in (A.8), which comes from the $\Gamma\left(\gamma+\gamma_1+\gamma_2-\frac{3}{2}\right)$ term in the second term on the RHS, in the case where $\gamma+\gamma_1+\gamma_2\to\frac{3}{2}$. This corresponds to the region where $|\nu|=0$, $|\nu_1|=0$ and $|\nu_2|=0$, or when $\gamma+\gamma_1+\gamma_2=-n$, where n is any real positive integer. However, as was mentioned above, it will be shown in Sect. A.2 that this region gives a vanishing contribution to the first enhanced amplitude, when it comes to integrating over the two rapidity variables Y_1 and Y_2 (see (39)) for the region close to the points $|\nu_1|\to 0$ and $|\nu_2|\to 0$. Therefore, this singularity never becomes manifest in the calculation, and hence in the only relevant case when $\mathrm{i}\nu\to\frac{1}{2}$ and $|\nu_1|,|\nu_2|\to 0$. Even though the first term on the RHS of (A.8) is thrown away, this singularity, namely when $\gamma+\gamma_1+\gamma_2\to 3/2$, is not lost. Hence, (A.8) reduces to

$$\int\frac{\mathrm{d}R'}{\left(R'_+\right)^{\gamma_2}\left(R'_-\right)^{\gamma_2}}\left(R_--R'_-\right)^{\gamma+\gamma_1+\gamma_2-2}=$$
$$\pi^{-\frac{1}{2}}\Gamma(2-\gamma-\gamma_1-\gamma_2)\Gamma\left(\gamma+\gamma_1+\gamma_2-\frac{3}{2}\right)x_-^{(\gamma+\gamma_1+\gamma_2)-2}\,. \tag{A.9}$$

Inserting the result of (A.9) back into the result of (A.4) gives

$$\begin{aligned}
&g_{3P}\left(\gamma,\gamma_1,\gamma_2\right)\\
&\quad=\int\frac{\mathrm{d}R_+}{R_+^{\gamma_2}}\int\mathrm{d}x_+\frac{(x_+-n)^{\gamma+\gamma_1+\gamma_2-2}}{x_+^{\gamma_1}(x_+-n)^{\gamma_2}(R_+-x_+)^{\gamma_2}}\\
&\quad\times\int\frac{\mathrm{d}\left(R_+^*\right)}{\left(R_+^*\right)^{\gamma_2}}\int\mathrm{d}\left(x_+^*\right)\\
&\quad\times\frac{\left(\left(x_+^*\right)-n\right)^{\gamma+\gamma_1+\gamma_2-2}}{\left(x_+^*\right)^{\gamma_1}\left(\left(x_+^*\right)-n\right)^{\gamma_2}\left(\left(R_+^*\right)-\left(x_+^*\right)\right)^{\gamma_2}}\\
&\quad\times\frac{1}{\pi}\Gamma^2(2-\gamma-\gamma_1-\gamma_2)\Gamma^2\left(\gamma+\gamma_1+\gamma_2-\frac{3}{2}\right)\,.
\end{aligned}\tag{A.10}$$

Now, using the notation for γ, γ_1 and γ_2 defined in (A.5), $g_{3P}(\gamma,\gamma_1,\gamma_2)$ becomes, in the limit that $|\nu_1|=|\nu_2|=0$,

$$\begin{aligned}
g_{3P}(\gamma,\gamma_1,\gamma_2)&=\lim_{\mathrm{i}\nu_1\to 0}\int\frac{\mathrm{d}R_+}{R_+^{\frac{1}{2}+\mathrm{i}\nu_1}}\\
&\times\int\mathrm{d}x_+\frac{1}{x_+^{\frac{1}{2}+\mathrm{i}\nu_1}(x_+-n)^{\frac{1}{2}-3\mathrm{i}\nu_1}(R_+-x_+)^{\frac{1}{2}+\mathrm{i}\nu_1}}\\
&\times\lim_{\mathrm{i}\nu_2\to 0}\int\frac{\mathrm{d}R_+^*}{\left(R_+^*\right)^{\frac{1}{2}+\mathrm{i}\nu_2}}\int\mathrm{d}x_+^*\\
&\times\frac{1}{\left(x_+^*\right)^{\frac{1}{2}+\mathrm{i}\nu_2}\left(x_+^*-n\right)^{\frac{1}{2}-3\mathrm{i}\nu_2}\left(R_+^*-x_+^*\right)^{\frac{1}{2}+\mathrm{i}\nu_2}}\\
&\times\frac{1}{\pi}\Gamma^2\left(\frac{1}{2}-\mathrm{i}\nu\right)\Gamma^2\left(\mathrm{i}\nu\right)\,.
\end{aligned}\tag{A.11}$$

It is instructive to leave ν_1 and ν_2 small but finite in the indices, and let them be driven to zero at the end of the calculation, to avoid divergent integrals. Now integrating over x_+ and x_+^* gives the following result:

$$\begin{aligned}
g_{3P}(\gamma,\gamma_1,\gamma_2)&=\frac{1}{\pi}\Gamma^2\left(\frac{1}{2}-\mathrm{i}\nu\right)\Gamma^2(\mathrm{i}\nu)\lim_{\mathrm{i}\nu_1\to 0}\int\frac{\mathrm{d}R_+}{R_+^{1+2\mathrm{i}\nu_1}}\\
&\times\frac{\Gamma\left(\frac{1}{2}+\mathrm{i}\nu_1\right)\Gamma\left(\frac{1}{2}+3\mathrm{i}\nu_1\right)}{\Gamma(1+4\mathrm{i}\nu_1)}{}_2F_1\\
&\times\left(\frac{1}{2}+\mathrm{i}\nu_1,\frac{1}{2}+\mathrm{i}\nu_1,1+4\mathrm{i}\nu_1,\frac{1}{R_+}\right)+R_+^{1+2\mathrm{i}\nu_1}\pi_2F_1\\
&\times\left(\frac{1}{2}-3\mathrm{i}\nu_1,\frac{1}{2}+\mathrm{i}\nu_1,1,R_+\right)\lim_{\mathrm{i}\nu_2\to 0}\int\frac{\mathrm{d}R_+^*}{\left(R_+^*\right)^{1+2\mathrm{i}\nu_2}}\\
&\times\frac{\Gamma\left(\frac{1}{2}+\mathrm{i}\nu_2\right)\Gamma\left(\frac{1}{2}+3\mathrm{i}\nu_2\right)}{\Gamma(1+4\mathrm{i}\nu_2)}{}_2F_1\\
&\times\left(\frac{1}{2}+\mathrm{i}\nu_2,\frac{1}{2}+\mathrm{i}\nu_2,1+4\mathrm{i}\nu_2,\frac{1}{R_+^*}\right)+\left(R_+^*\right)^{1+2\mathrm{i}\nu_2}\pi_2F_1\\
&\times\left(\frac{1}{2}-3\mathrm{i}\nu_2,\frac{1}{2}+\mathrm{i}\nu_2,1,R_+^*\right)\,.
\end{aligned}\tag{A.12}$$

In the limit that $|\nu_1|,|\nu_2|\to 0$ the factor

$$\frac{\Gamma\left(\frac{1}{2}+\mathrm{i}\nu_1\right)\Gamma\left(\frac{1}{2}+3\mathrm{i}\nu_1\right)}{\Gamma\left(1+4\mathrm{i}\nu_1\right)}\to\pi\,,$$

and (A.12) reduces to

$$\begin{aligned}
g_{3P}(\gamma,\gamma_1,\gamma_2)=\lim_{\mathrm{i}\nu_1\to 0}\int\frac{\mathrm{d}R_+}{R_+^{1+2\mathrm{i}\nu_1}}&\left({}_2F_1\left(\frac{1}{2},\frac{1}{2},1,\frac{1}{R_+}\right)\right.\\
&\left.+R_+^{1+2\mathrm{i}\nu_1}{}_2F_1\left(\frac{1}{2},\frac{1}{2},1,R_+\right)\right)\\
\times\lim_{\mathrm{i}\nu_2\to 0}\int\frac{\mathrm{d}R_+^*}{\left(R_+^*\right)^{1+2\mathrm{i}\nu_2}}&\left({}_2F_1\left(\frac{1}{2},\frac{1}{2},1,\frac{1}{R_+^*}\right)\right.\\
&\left.+\left(R_+^*\right)^{1+2\mathrm{i}\nu_2}{}_2F_1\left(\frac{1}{2},\frac{1}{2},1,R_+^*\right)\right)\\
&\times\pi\Gamma^2\left(\frac{1}{2}-\mathrm{i}\nu\right)\Gamma^2\left(\mathrm{i}\nu\right)\,.
\end{aligned}\tag{A.13}$$

Finally, evaluating the integral over R_+ in (A.13) gives the result for $g_{3P}\left(\gamma,\gamma_1,\gamma_2\right)$:

$$g_{3P}(\gamma,\gamma_1,\gamma_2)=\frac{1}{4\nu_1 4\nu_2\pi}\Gamma^2\left(\frac{1}{2}-\mathrm{i}\nu\right)\Gamma^2\left(\mathrm{i}\nu\right)\,. \tag{A.14}$$

Substituting this result for $g_{3P}(\gamma,\gamma_1,\gamma_2)$ of (A.14) into the expression of (A.3), the triple pomeron vertex is given explicitly in the momentum representation, in the limit that $|\nu_1|=|\nu_2|=0$, by the expression

$$\begin{aligned}
&G_{3P}(\mathbf{q}=0,\mathbf{k},\nu,\nu_1\to 0,\nu_2\to 0)=\\
&\frac{2^{-2\mathrm{i}\nu}}{4\nu_1 4\nu_2\pi}(k^2)^{\mathrm{i}\nu-\frac{1}{2}}\frac{\Gamma^3(\frac{1}{2}-\mathrm{i}\nu)\Gamma^2(\mathrm{i}\nu)}{\Gamma\left(\frac{1}{2}+\mathrm{i}\nu\right)}\,.
\end{aligned}\tag{A.15}$$

To calculate the first enhanced amplitude of Fig. 7, there is an integration to be evaluated of the two triple

pomeron vertices at both ends of the loop, over the unknown momentum $\mathbf{k}$ (see (39)), which takes the form

$$\int \mathrm{d}^2k G_{3P}(\mathbf{q}=0,\mathbf{k},\nu,\nu_1,\nu_2)G_{3P}(\mathbf{q}=0,\mathbf{k},-\nu',\nu_1,\nu_2)\,. \tag{A.16}$$

Inserting the result of (A.15) gives

$$\begin{aligned}&\int \mathrm{d}^2k G_{3P}(\mathbf{q}=0,\mathbf{k},\nu,\nu_1,\nu_2)G_{3P}(-\nu',\nu_1,\nu_2)\\&=\frac{2^{2(\mathrm{i}\nu'-\mathrm{i}\nu)}}{\pi^2}\int \mathrm{d}^2k(k^2)^{(\mathrm{i}\nu-\mathrm{i}\nu')-1}\\&\times\frac{\Gamma^3\left(\frac{1}{2}-\mathrm{i}\nu\right)\Gamma^3\left(\frac{1}{2}+\mathrm{i}\nu'\right)\Gamma^2(\mathrm{i}\nu)\Gamma^2(-\mathrm{i}\nu')}{\Gamma\left(\frac{1}{2}+\mathrm{i}\nu\right)\Gamma\left(\frac{1}{2}-\mathrm{i}\nu'\right)}\frac{1}{16\nu_1^2 16\nu_2^2}\,.\end{aligned} \tag{A.17}$$

Now to integrate over k, it is useful to make the change of variable $l=\ln k$. Then the right hand side of (A.17) reduces to a delta function in ν and ν', to give the result

$$\begin{aligned}&\int \mathrm{d}^2k G_{3P}(\mathbf{q}=0,\mathbf{k},\nu,\nu_1,\nu_2)G_{3P}(-\nu',\nu_1,\nu_2)=\\&\frac{2^{2(\mathrm{i}\nu'-\mathrm{i}\nu)}}{8}\frac{\delta(\nu-\nu')}{4\nu_1^2 4\nu_2^2}\\&\times\frac{\Gamma^3\left(\frac{1}{2}-\mathrm{i}\nu\right)\Gamma^3\left(\frac{1}{2}+\mathrm{i}\nu'\right)\Gamma^2(\mathrm{i}\nu)\Gamma^2(-\mathrm{i}\nu')}{\Gamma\left(\frac{1}{2}+\mathrm{i}\nu\right)\Gamma\left(\frac{1}{2}-\mathrm{i}\nu'\right)}\,.\end{aligned} \tag{A.18}$$

A.2 Calculation of the first enhanced amplitude

In this subsection, the amplitude for the first enhanced diagram is derived by evaluating the integrals on the RHS of (39), namely

$$\begin{aligned}P^{\mathrm{BFKL}}_{\mathrm{enhanced}}(\mathbf{p}_1,\mathbf{p}_2,Y,\mathbf{q})&=B\int_{-\infty}^{\infty}\mathrm{d}\nu\int_{-\infty}^{\infty}\mathrm{d}\nu'\int_{-\infty}^{\infty}\mathrm{d}\nu_1\\&\times\int_{-\infty}^{\infty}\mathrm{d}\nu_2\int\mathrm{d}^2k\int_{Y_{\mathrm{H}}+\frac{1}{2}\delta Y_{\mathrm{H}}}^{Y}\mathrm{d}Y_1\int_0^{Y_{\mathrm{H}}-\frac{1}{2}\delta Y_{\mathrm{H}}}\mathrm{d}Y_2\\&\times E(\mathbf{p}_1,\mathbf{q},\nu)\mathcal{D}(\nu)\mathrm{e}^{\omega(\nu)(Y-Y_1)}G_{3P}(\nu,\nu_1,\nu_2,\mathbf{q}=0,\mathbf{k})\\&\times\mathcal{D}(\nu_1)\mathcal{D}(\nu_2)\mathrm{e}^{(\omega(\nu_1)+\omega(\nu_2))(Y_1-Y_2)-\omega(\nu_2)\delta Y_{\mathrm{H}}}\\&\times G_{3P}(-\nu',\nu_1,\nu_2,\mathbf{q}=0,\mathbf{k})\mathrm{e}^{\omega(\nu')Y_2}E(\mathbf{p}_2,\mathbf{q},-\nu')\,.\end{aligned} \tag{A.19}$$

There are three regions of integration to be considered, namely the region close to $|\nu|\to 0$ and the region close to $\mathrm{i}\nu\to\pm\frac{1}{2}$. Firstly, the regions close to $\mathrm{i}\nu\to\pm\frac{1}{2}$ will be considered at the same time, because as will be shown, it turns out that, in fact, the integration over ν is the same around these two points. Integrating the product of the two triple pomeron vertices appearing in (A.19) over the unknown momentum $\mathbf{k}$ in the loop results in the expression given in (A.18), which is proportional to the Dirac delta function $\delta(\nu-\nu')$. Inserting this into the RHS of (A.19), and absorbing the delta function $\delta(\nu-\nu')$ by integrating over ν' and setting everywhere $\nu=\nu'$ results in the expression

$$\begin{aligned}P^{\mathrm{BFKL}}_{\mathrm{enhanced}}&=\frac{B}{8}\int_{-\infty}^{\infty}\mathrm{d}\nu\int_{-\infty}^{\infty}\mathrm{d}\nu_1\int_{-\infty}^{\infty}\mathrm{d}\nu_2\int_{Y_{\mathrm{H}}+\frac{1}{2}\delta Y_{\mathrm{H}}}^{Y}\mathrm{d}Y_1\\&\times\int_0^{Y_{\mathrm{H}}-\frac{1}{2}\delta Y_{\mathrm{H}}}\mathrm{d}Y_2E(\mathbf{p}_1,\mathbf{q},\nu)\mathcal{D}^2(\nu)\mathrm{e}^{\omega(\nu)(Y-Y_1+Y_2)}\\&\times\frac{\Gamma^3\left(\frac{1}{2}-\mathrm{i}\nu\right)\Gamma^3\left(\frac{1}{2}+\mathrm{i}\nu\right)\Gamma^2(\mathrm{i}\nu)\Gamma^2(-\mathrm{i}\nu)}{4\nu_1^2 4\nu_2^2\Gamma\left(\frac{1}{2}+\mathrm{i}\nu\right)\Gamma\left(\frac{1}{2}-\mathrm{i}\nu\right)}\\&\times\mathcal{D}(\nu_1)\mathcal{D}(\nu_2)\mathrm{e}^{(\omega(\nu_1)+\omega(\nu_2))(Y_1-Y_2)-\omega(\nu_2)\delta Y_{\mathrm{H}}}E(\mathbf{p}_2,\mathbf{q},-\nu)\,,\end{aligned} \tag{A.20}$$

where

$$B=-\frac{\alpha_{\mathrm{s}}^4\pi^4}{8}\left(\frac{\alpha_{\mathrm{s}}N_c}{2\pi^2}\right)^2\,.$$

Using the identity $\Gamma(x)\Gamma(1-x)=\pi/\sin\pi x$, the integrand of (A.20) simplifies to

$$\begin{aligned}P^{\mathrm{BFKL}}_{\mathrm{enhanced}}&=\frac{B\pi^2}{8}\int_{-\infty}^{\infty}\mathrm{d}\nu\int_{-\infty}^{\infty}\mathrm{d}\nu_1\int_{-\infty}^{\infty}\mathrm{d}\nu_2\int_{Y_{\mathrm{H}}+\frac{1}{2}\delta Y_{\mathrm{H}}}^{Y}\mathrm{d}Y_1\\&\times\int_0^{Y_{\mathrm{H}}-\frac{1}{2}\delta Y_{\mathrm{H}}}\mathrm{d}Y_2E(\mathbf{p}_1,\mathbf{q},\nu)\mathcal{D}^2(\nu)\mathrm{e}^{\omega(\nu)(Y-Y_1+Y_2)}\\&\times\frac{\Gamma^2\left(\frac{1}{2}-\mathrm{i}\nu\right)\Gamma^2\left(\frac{1}{2}+\mathrm{i}\nu\right)}{4\nu_1^2 4\nu_2^2\nu^2\sin^2(\mathrm{i}\nu\pi)}\mathcal{D}(\nu_1)\mathcal{D}(\nu_2)\\&\times\mathrm{e}^{(\omega(\nu_1)+\omega(\nu_2))(Y_1-Y_2)-\omega(\nu_2)\delta Y_{\mathrm{H}}}E(\mathbf{p}_2,\mathbf{q},-\nu)\,.\end{aligned} \tag{A.21}$$

It is assumed that the conjugate momenta $\mathbf{p}_1$ and $\mathbf{p}_2$ of the two scattering dipoles in Fig. 7 are equal. Using the expression of (18) for the two pomeron vertices, (A.21) reduces to

$$\begin{aligned}P^{\mathrm{BFKL}}_{\mathrm{enhanced}}&=\frac{2B\pi^6}{p^2}\int_{-\infty}^{\infty}\mathrm{d}\nu\int_{-\infty}^{\infty}\mathrm{d}\nu_1\int_{-\infty}^{\infty}\mathrm{d}\nu_2\int_{Y_{\mathrm{H}}+\frac{1}{2}\delta Y_{\mathrm{H}}}^{Y}\mathrm{d}Y_1\\&\times\int_0^{Y_{\mathrm{H}}-\frac{1}{2}\delta Y_{\mathrm{H}}}\mathrm{d}Y_2\mathcal{D}^2(\nu)\mathrm{e}^{\omega(\nu)(Y-Y_1+Y_2)}\\&\times\frac{\Gamma^2\left(\frac{1}{2}-\mathrm{i}\nu\right)\Gamma^2\left(\frac{1}{2}+\mathrm{i}\nu\right)}{4\nu_1^2 4\nu_2^2\nu^4\sin^2(\mathrm{i}\nu\pi)}\\&\times\mathcal{D}(\nu_1)\mathcal{D}(\nu_2)\mathrm{e}^{(\omega(\nu_1)+\omega(\nu_2))(Y_1-Y_2)-\omega(\nu_2)\delta Y_{\mathrm{H}}}\,.\end{aligned} \tag{A.22}$$

Hence the expression on the RHS of (A.19) reduces to the product of integrals over ν, ν_1 and ν_2, as well as the integrations over the rapidity variables Y_1 and Y_2, which can be written in the simplified form

$$P^{\mathrm{BFKL}}_{\mathrm{enhanced}}=\frac{2B\pi^6}{p^2}\int_{Y_{\mathrm{H}}+\frac{1}{2}\delta Y_{\mathrm{H}}}^{Y}\mathrm{d}Y_1\int_0^{Y_{\mathrm{H}}-\frac{1}{2}\delta Y_{\mathrm{H}}}\mathrm{d}Y_2I_\nu I_{\nu_1}I_{\nu_2}\,, \tag{A.23}$$

where

$$I_\nu = \int_{-\infty}^{\infty} \mathrm{d}\nu \mathrm{e}^{\omega(\nu)(Y-Y_1+Y_2)} \times \frac{\Gamma^2\left(\frac{1}{2}-\mathrm{i}\nu\right)\Gamma^2\left(\frac{1}{2}+\mathrm{i}\nu\right)D^2(\nu)}{\sin^2(\mathrm{i}\nu\pi)\nu^4}, \quad \text{(A.24)}$$

$$I_{\nu_1} = \int_{-\infty}^{\infty} \mathrm{d}\nu_1 \frac{\mathrm{e}^{\omega(\nu_1)(Y_1-Y_2)}D(\nu_1)}{4}, \quad \text{(A.25)}$$

$$I_{\nu_2} = \int_{-\infty}^{\infty} \mathrm{d}\nu_2 \frac{\mathrm{e}^{\omega(\nu_2)(Y_1-Y_2)}D(\nu_2)}{4}. \quad \text{(A.26)}$$

Consider first the integration over γ in (A.21). Recall that the definition of the BFKL eigenvalue, namely $\omega(\nu) = \bar{\alpha}_\mathrm{s}\left\{\psi(1) - \psi\left(\frac{1}{2}+\mathrm{i}\nu\right) - \left(\frac{1}{2}-\mathrm{i}\nu\right)\right\}$, which has two poles at the points where $\nu \to \pm\frac{1}{2}$. In these cases, the BFKL eigenvalue behaves as

$$\omega(\nu) \xrightarrow{\nu\to\pm\frac{1}{2}} -\frac{2\bar{\alpha}_\mathrm{s}}{\frac{1}{2}\pm\mathrm{i}\nu}. \quad \text{(A.27)}$$

The rest of the ν dependent part of the integrand, namely $\frac{\Gamma^2\left(\frac{1}{2}-\mathrm{i}\nu\right)\Gamma^2\left(\frac{1}{2}+\mathrm{i}\nu\right)D^2(\nu)}{\sin^2(\mathrm{i}\nu\pi)\nu^4}$ behaves like

$$\frac{\Gamma^2\left(\frac{1}{2}-\mathrm{i}\nu\right)\Gamma^2\left(\frac{1}{2}+\mathrm{i}\nu\right)D^2(\nu)}{\sin^2(\mathrm{i}\nu\pi)\nu^4} \xrightarrow{\nu\to\pm\frac{1}{2}} \left(\frac{1}{2}\pm\mathrm{i}\nu\right)^{-6}, \quad \text{(A.28)}$$

where the fact that the Euler gamma function $\Gamma(x) \xrightarrow{x\to 0} x^{-1}$ has been used in (A.28). Therefore, plugging (A.28) into (A.24), the ν part of the integration in (A.21) at these two poles takes the form

$$I_\nu \xrightarrow{\nu\to\pm\frac{1}{2}} \int_{-\infty}^{\infty} \mathrm{d}\nu \frac{\exp\left(-\frac{2\bar{\alpha}_\mathrm{s}}{\frac{1}{2}\pm\mathrm{i}\nu}(Y-Y_1+Y_2)\right)}{\left(\frac{1}{2}\pm\mathrm{i}\nu\right)^6} = \frac{1}{(2\bar{\alpha}_\mathrm{s})^4}\frac{\mathrm{d}^4}{\mathrm{d}Y^4}\int_{-\infty}^{\infty} \mathrm{d}\nu \frac{\exp\left(-\frac{2\bar{\alpha}_\mathrm{s}}{\left(\frac{1}{2}\pm\mathrm{i}\nu\right)}(Y-Y_1+Y_2)\right)}{\left(\frac{1}{2}\pm\mathrm{i}\nu\right)^2}. \quad \text{(A.29)}$$

At this stage, it is instructive to change the variables in (A.29) to $-\mathrm{i}u = -\frac{2\bar{\alpha}_\mathrm{s}}{\frac{1}{2}\pm\mathrm{i}\nu}$. The integration measure becomes

$$\int_{-\infty}^{\infty} \mathrm{d}\nu \to 2\bar{\alpha}_\mathrm{s}\int_{-\infty}^{\infty}\frac{\mathrm{d}u}{u^2}. \quad \text{(A.30)}$$

Then (A.29) becomes in the terms of the new integration variables

$$I_\nu \xrightarrow{\nu\to\pm\frac{1}{2}} \frac{-1}{(2\bar{\alpha}_\mathrm{s})^5}\frac{\mathrm{d}^4}{\mathrm{d}Y^4}\int_{-\infty}^{+\infty}\mathrm{d}u\mathrm{e}^{(Y-Y_1+Y_2)u} \quad \text{(A.31)}$$

$$= \frac{2\pi}{(2\bar{\alpha}_\mathrm{s})^5}\frac{\mathrm{d}^4}{\mathrm{d}Y^4}\delta(Y-Y_1+Y_2). \quad \text{(A.32)}$$

Inserting (A.32) into (A.21) gives the expression for the amplitude of the first enhanced diagram as $\mathrm{i}\nu \to \pm\frac{1}{2}$:

$$[P^{\mathrm{BFKL}}_{\mathrm{enhanced}}]_{\mathrm{i}\nu\to\pm\frac{1}{2}} = \frac{2B\pi^6}{p^2}\frac{\pi}{(2\bar{\alpha}_\mathrm{s})^5}\frac{\mathrm{d}^4}{\mathrm{d}Y^4}\int_{Y_\mathrm{H}+\frac{1}{2}\delta Y_\mathrm{H}}^{Y}\mathrm{d}Y_1 \times \int_0^{Y_\mathrm{H}-\frac{1}{2}\delta Y_\mathrm{H}}\mathrm{d}Y_2\delta(Y-Y_1+Y_2)I_{\nu_1}I_{\nu_2}. \quad \text{(A.33)}$$

The integrations over ν_1 and ν_2 given in (A.25) and (A.26) also contain three significant regions of integration, namely, the regions close to $\mathrm{i}\nu_i \to \pm\frac{1}{2}$ and $|\nu_i| \to 0$ $(i = 1, 2)$. The following argument will show that the regions close to the points as $\mathrm{i}\nu_i \to \pm\frac{1}{2}$ give a vanishing contribution to the amplitude of the first enhanced diagram. This is because inserting $I_{\mathrm{i}\nu_i\to\pm\frac{1}{2}}$ into (A.21), the integration over the rapidity variables vanishes, as will be shown below. Following this, I_{ν_1} and I_{ν_2} will be evaluated in this section for the most important region, namely close to the point when $|\nu_i| \to 0$ $(i = 1, 2)$. Using the relation of (A.27), in the region close to $\mathrm{i}\nu_i \to \pm\frac{1}{2}$, I_{ν_1} and I_{ν_2} given in (A.25) and (A.26) behave like

$$I_{\mathrm{i}\nu_1\to\pm\frac{1}{2}} = \int_{-\infty}^{\infty}\mathrm{d}\nu_1\frac{1}{4}\frac{\exp\left(-\frac{2\bar{\alpha}_\mathrm{s}}{\frac{1}{2}\pm\mathrm{i}\nu_1}(Y_1-Y_2)\right)}{\frac{1}{2}\pm\mathrm{i}\nu_2},$$

$$I_{\mathrm{i}\nu_2\to\pm\frac{1}{2}} = \int_{-\infty}^{\infty}\mathrm{d}\nu_2\frac{1}{4}\frac{\exp\left(-\frac{2\bar{\alpha}_\mathrm{s}}{\frac{1}{2}\pm\mathrm{i}\nu_2}(Y_1-Y_2-\delta Y_\mathrm{H})\right)}{\left(\frac{1}{2}\pm\mathrm{i}\nu_2\right)^2}. \quad \text{(A.34)}$$

Using the same change of variables invoked in (A.30), (A.34) becomes

$$I_{\mathrm{i}\nu_1\to\pm\frac{1}{2}} = \frac{1}{2\bar{\alpha}_\mathrm{s}}\int_{-\infty}^{\infty}\mathrm{d}u\frac{1}{4}\exp((Y_1-Y_2)u) = \frac{\pi}{2\bar{\alpha}_\mathrm{s}}\delta(Y_1-Y_2), \quad \text{(A.35)}$$

$$I_{\mathrm{i}\nu_2\to\pm\frac{1}{2}} = \frac{1}{2\bar{\alpha}_\mathrm{s}}\int_{-\infty}^{\infty}\mathrm{d}u\frac{1}{4}\exp((Y_1-Y_2-\delta Y_\mathrm{H})u) = \frac{\pi}{2\bar{\alpha}_\mathrm{s}}\delta(Y_1-Y_2-\delta Y_\mathrm{H}). \quad \text{(A.36)}$$

However, due to the Dirac delta function on the RHS, it is obvious that inserting $I_{\nu_1\to\pm\frac{1}{2}}$ into (A.33) we obtain the expression

$$[P^{\mathrm{BFKL}}_{\mathrm{enhanced}}]_{\mathrm{i}\nu_1\to\pm\frac{1}{2}} = \frac{B\pi^6}{p^2}\int_{Y_\mathrm{H}+\delta Y_\mathrm{H}}^{Y}\mathrm{d}Y_1\int_0^{Y_\mathrm{H}-\delta Y_\mathrm{H}}\mathrm{d}Y_2 I_\nu\frac{\pi}{\bar{\alpha}_\mathrm{s}}\delta(Y_1-Y_2)I_{\nu_2}. \quad \text{(A.37)}$$

The integration over the rapidity variables Y_1 and Y_2 vanishes in (A.37). The reason for this is that from the limits of the integration over the rapidity variables in (A.37), one deduces the inequality condition $Y_1 - Y_2 \geq \delta Y_\mathrm{H}$. Hence, the argument of the delta function is never zero within the

specified region of integration. Therefore, the integration over the rapidity variables Y_1 and Y_2 on the RHS of (A.37) vanishes, and one can conclude that the region close to the points when $\nu_i \to \pm\frac{1}{2}$ does not contribute to the integration at all.

Now that it has been argued that I_{ν_1} and I_{ν_2} do not contribute in the regions close to the points $\mathrm{i}\nu_i \to \pm\frac{1}{2}$, the main contribution of the I_{ν_i} when $|\nu_i| \to 0$ will now be derived. As $|\nu_i| \to 0$, the BFKL eigenvalue in the exponential of (A.25) and (A.26) has a saddle point. Hence, one can expand $\omega(\nu_i)$ in powers of ν_i around the saddle point $\nu_i = 0$ as

$$\omega(\nu_i) = \omega(0) + \frac{1}{2}\nu_i^2\omega''(0)\,, \tag{A.38}$$

where in (A.38) only powers as high as ν_i^2 in the expansion are considered, since the BFKL eigenvalue $\omega(\nu_i)$ decreases in value as the value of ν_i increases. Hence, one is justified in neglecting powers higher than ν_i^2 for small values of ν_i. Using the expansion of (A.38), $I_{|\nu_1|\to 0}$ and $I_{|\nu_2|\to 0}$ take the form

$$I_{|\nu_1|\to 0} = 4\int_{-\infty}^{\infty} \mathrm{d}\nu_1 \mathrm{e}^{\omega(0)(Y_1-Y_2)+\frac{1}{2}\nu_1^2\omega''(0)(Y_1-Y_2)}\,, \tag{A.39}$$

$$I_{|\nu_2|\to 0} = 4\int_{-\infty}^{\infty} \mathrm{d}\nu_2 \mathrm{e}^{\omega(0)(Y_1-Y_2-\delta Y_{\mathrm{H}})+\frac{1}{2}\nu_2^2\omega''(0)(Y_1-Y_2-\delta Y_{\mathrm{H}})}. \tag{A.40}$$

Noting that the exponential in (A.39) and (A.40) has a saddle point at $\nu_1 = 0$ and $\nu_2 = 0$, one can integrate over ν_1 and ν_2 using the method of steepest descent to give the results

$$I_{|\nu_1|\to 0} = 4\left(\frac{-2\pi}{\omega''(0)(Y_1-Y_2)}\right)^{1/2} \mathrm{e}^{\omega(0)(Y_1-Y_2)}\,, \tag{A.41}$$

$$I_{|\nu_2|\to 0} = 4\left(\frac{-2\pi}{\omega''(0)(Y_1-Y_2-\delta Y_{\mathrm{H}})}\right)^{1/2} \mathrm{e}^{\omega(0)(Y_1-Y_2-\delta Y_{\mathrm{H}})}\,. \tag{A.42}$$

Finally inserting the results of (A.41) and (A.42) into (A.33) gives the result

$$\begin{aligned}[P^{\mathrm{BFKL}}_{\mathrm{enhanced}}]_{\nu\to\pm\frac{1}{2}} &= \frac{32B\pi^7}{p^2}\frac{1}{(2\bar{\alpha}_{\mathrm{s}})^5}\frac{\mathrm{d}^4}{\mathrm{d}Y^4} \\ &\times\left\{\int_{Y_{\mathrm{H}}+\frac{1}{2}\delta Y_{\mathrm{H}}}^{Y}\mathrm{d}Y_1\int_0^{Y_{\mathrm{H}}-\frac{1}{2}\delta Y_{\mathrm{H}}}\mathrm{d}Y_2\delta(Y-Y_1+Y_2)\right. \\ &\left.\times\frac{2\pi\mathrm{e}^{2\omega(0)(Y_1-Y_2-\frac{1}{2}\delta Y_{\mathrm{H}})}}{\omega''(0)(Y_1-Y_2)^{1/2}(Y_1-Y_2-\delta Y_{\mathrm{H}})^{1/2}}\right\}. \end{aligned} \tag{A.43}$$

Now that the result for the first enhanced diagram for the region close to $\mathrm{i}\nu \to \pm\frac{1}{2}$ has been derived, the last region to consider is the contribution from the region close to $|\nu| \to 0$. Returning to (A.20), the expression for the amplitude of the first enhanced diagram is

$$\begin{aligned}P^{\mathrm{BFKL}}_{\mathrm{enhanced}}(\mathbf{p}_1,\mathbf{p}_2,Y,\mathbf{q}) &= B\int_{-\infty}^{\infty}\mathrm{d}\nu\int_{-\infty}^{\infty}\mathrm{d}\nu'\int_{-\infty}^{\infty}\mathrm{d}\nu_1 \\ &\times\int_{-\infty}^{\infty}\mathrm{d}\nu_2\int_{Y_{\mathrm{H}}+\frac{1}{2}\delta Y_{\mathrm{H}}}^{Y}\mathrm{d}Y_1\int_0^{Y_{\mathrm{H}}-\frac{1}{2}\delta Y_{\mathrm{H}}}\mathrm{d}Y_2 \\ &\times E(\mathbf{p}_1,\mathbf{q},\nu)\mathcal{D}(\nu)\mathrm{e}^{\omega(\nu)(Y-Y_1)}\mathcal{D}(\nu_1)\mathcal{D}(\nu_2) \\ &\times\mathrm{e}^{(\omega(\nu_1)+\omega(\nu_2))(Y_1-Y_2)-\omega(\nu_2)\delta Y_{\mathrm{H}}}\mathrm{e}^{\omega(\nu')Y_2}E(\mathbf{p}_2,\mathbf{q},-\nu') \\ &\times\frac{2^{2(\mathrm{i}\nu'-\mathrm{i}\nu)}}{8}\frac{\delta(\nu-\nu')}{4\nu_1^2 4\nu_2^2} \\ &\times\frac{\Gamma^3\left(\frac{1}{2}-\mathrm{i}\nu\right)\Gamma^3\left(\frac{1}{2}+\mathrm{i}\nu'\right)\Gamma^2(\mathrm{i}\nu)\Gamma^2(-\mathrm{i}\nu')}{\Gamma\left(\frac{1}{2}+\mathrm{i}\nu\right)\Gamma\left(\frac{1}{2}-\mathrm{i}\nu'\right)}\,. \end{aligned} \tag{A.44}$$

Now taking the limit that $|\nu| \to 0$, this expression simplifies to

$$\begin{aligned}P^{\mathrm{BFKL}}_{\mathrm{enhanced}}(\mathbf{p}_1,\mathbf{p}_2,Y,\mathbf{q}) &\xrightarrow{|\nu|\to 0} \frac{B\pi^2}{8}\int_{-\infty}^{\infty}\mathrm{d}\nu\int_{-\infty}^{\infty}\mathrm{d}\nu_1 \\ &\times\int_{-\infty}^{\infty}\mathrm{d}\nu_2\int_{Y_{\mathrm{H}}+\frac{1}{2}\delta Y_{\mathrm{H}}}^{Y}\mathrm{d}Y_1\int_0^{Y_{\mathrm{H}}-\frac{1}{2}\delta Y_{\mathrm{H}}}\mathrm{d}Y_2 \\ &\times E(\mathbf{p}_1,\mathbf{q},\nu)\mathcal{D}^2(\nu)\mathrm{e}^{\omega(\nu)(Y-Y_1+Y_2)}\frac{\mathcal{D}(\nu_1)\mathcal{D}(\nu_2)}{4\nu_1^2 4\nu_2^2\nu^4} \\ &\times\mathrm{e}^{(\omega(\nu_1)+\omega(\nu_2))(Y_1-Y_2)-\omega(\nu_2)\delta Y_{\mathrm{H}}}E(\mathbf{p}_2,\mathbf{q},-\nu)\,. \end{aligned} \tag{A.45}$$

It is assumed that the conjugate momenta $\mathbf{p}_1$ and $\mathbf{p}_2$ of the two scattering dipoles in Fig. 7 are equal. Using the expression of (18) for the two pomeron vertices, (A.45) reduces to

$$\begin{aligned}[P^{\mathrm{BFKL}}_{\mathrm{enhanced}}(\mathbf{p}_1=\mathbf{p}_2=\mathbf{p},Y,\mathbf{q})]_{|\nu|\to 0} &= \frac{2B\pi^6}{p^2}\int_{-\infty}^{\infty}\mathrm{d}\nu \\ &\times\int_{-\infty}^{\infty}\mathrm{d}\nu_1\int_{-\infty}^{\infty}\mathrm{d}\nu_2\int_{Y_{\mathrm{H}}+\frac{1}{2}\delta Y_{\mathrm{H}}}^{Y}\mathrm{d}Y_1\int_0^{Y_{\mathrm{H}}-\frac{1}{2}\delta Y_{\mathrm{H}}}\mathrm{d}Y_2 \\ &\times\mathcal{D}^2(\nu)\mathrm{e}^{\omega(\nu)(Y-Y_1+Y_2)}\frac{\mathcal{D}(\nu_1)\mathcal{D}(\nu_2)}{4\nu_1^2 4\nu_2^2\nu^4} \\ &\times\mathrm{e}^{(\omega(\nu_1)+\omega(\nu_2))(Y_1-Y_2)-\omega(\nu_2)\delta Y_{\mathrm{H}}} = \frac{2B\pi^6}{p^2}\int_{-\infty}^{\infty}\mathrm{d}\nu \\ &\times\int_{-\infty}^{\infty}\mathrm{d}\nu_1\int_{-\infty}^{\infty}\mathrm{d}\nu_2\int_{Y_{\mathrm{H}}+\frac{1}{2}\delta Y_{\mathrm{H}}}^{Y}\mathrm{d}Y_1 \\ &\times\int_0^{Y_{\mathrm{H}}-\frac{1}{2}\delta Y_{\mathrm{H}}}\mathrm{d}Y_2 I'_{|\nu|\to 0}I_{\nu_1}I_{\nu_2}\,, \end{aligned} \tag{A.46}$$

where

$$I'_{\nu} = \int_{-\mathrm{i}\infty+\epsilon}^{\mathrm{i}\infty+\epsilon}\mathrm{d}\gamma\frac{\mathrm{e}^{\omega(\nu)(Y-Y_1+Y_2)}D^2(\nu)}{\nu^4} \tag{A.47}$$

and I_{ν_1} and I_{ν_2} are given in (A.25) and (A.26). In the case when $|\nu| \to 0$, the BFKL eigenvalue $\omega(\nu)$ has a saddle point, such that one can use the expression given in (A.38)

for the BFKL eigenvalue $\omega(\nu)$ in (A.47). Hence, the integral I'_ν in the limit that $|\nu| \to 0$ takes the form

$$I'_{\nu\to 0} = 256 \mathrm{e}^{\omega(0)(Y-Y_1+Y_2)} \int_{-\infty}^{\infty} \mathrm{d}\nu \mathrm{e}^{\frac{1}{2}\nu^2\omega''(0)(Y-Y_1+Y_2)} = 256 \mathrm{e}^{\omega(0)(Y-Y_1+Y_2)} \left(\frac{2\pi}{\omega''(0)(Y-Y_1+Y_2)}\right)^{1/2}. \tag{A.48}$$

It was argued above that the only non-vanishing contributions to I_{ν_1} and I_{ν_2} were for the cases where $|\nu_1| \to 0$ and $|\nu_2| \to 0$, and the results for these regions are given in (A.41) and (A.42). Hence, inserting (A.48), together with (A.41) and (A.42) into (A.46) gives the result

$$\left[P^{\mathrm{BFKL}}_{\mathrm{enhanced}}(\mathbf{p}_1 = \mathbf{p}_2 = \mathbf{p}, Y, \mathbf{q})\right]_{|\nu|=\to 0} = \left(\frac{2\pi}{\omega''(0)}\right)^{3/2} \frac{512 B\pi^6}{p^2} \mathrm{e}^{\omega(0)Y} \int_{Y_{\mathrm{H}}+\frac{1}{2}\delta Y_{\mathrm{H}}}^{Y} \mathrm{d}Y_1 \times \int_0^{Y_{\mathrm{H}}-\frac{1}{2}\delta Y_{\mathrm{H}}} \mathrm{d}Y_2 \exp(\omega(0)(Y_1 - Y_2 - \delta Y_{\mathrm{H}})) \times 16 \left\{(Y_1 - Y_2)(Y_1 - Y_2 - \delta Y_{\mathrm{H}})(Y - Y_1 + Y_2)\right\}^{-1/2}. \tag{A.49}$$

Comparing this with (A.43), which was for the case of $\mathrm{i}\nu \to \pm\frac{1}{2}$, one notices a relative suppression of $\bar{\alpha}_{\mathrm{s}}^5$, as well as an extra term of the order of $\frac{1}{Y}$ after integration over the rapidity variables. Therefore, it turns out that the contribution coming from the region of integration close to the point $|\nu| \to 0$, namely $[P^{\mathrm{BFKL}}_{\mathrm{enhanced}}(\mathbf{p}_1 = \mathbf{p}_2 = \mathbf{p}, Y, \mathbf{q})]_{|\nu|=\to 0}$ given in (A.49), is small compared to $[P^{\mathrm{BFKL}}_{\mathrm{enhanced}}(\mathbf{p}_1 = \mathbf{p}_2 = \mathbf{p}, Y, \mathbf{q})]_{\mathrm{i}\nu=\to\pm\frac{1}{2}}$ given in (A.43). Therefore, neglecting this contribution when $|\nu| \to 0$, the result for the amplitude of the first enhanced diagram is given by the expression of (A.43). Using the delta function $\delta(Y - Y_1 + Y_2)$ in the integrand of (A.43), one can easily integrate over the rapidity variables. If one works in the chosen frame where the Higgs boson is produced at the rapidity value $Y_{\mathrm{H}} = 0$, the final expression for the amplitude of the first enhanced diagram takes the form

$$P^{\mathrm{BFKL}}_{\mathrm{enhanced}} = \frac{32B\pi^8}{p^2} \frac{1}{(2\bar{\alpha}_{\mathrm{s}})^5} \frac{\mathrm{d}^4}{\mathrm{d}Y^4} \left\{\frac{\mathrm{e}^{2\omega(0)(Y-\frac{1}{2}\delta Y_{\mathrm{H}})}\delta Y_{\mathrm{H}}}{\omega''(0) Y^{1/2}(Y-\delta Y_{\mathrm{H}})^{1/2}}\right\} = \frac{32B\pi^8}{p^2} \frac{1}{(2\bar{\alpha}_{\mathrm{s}})^5} \left\{\frac{\mathrm{e}^{2\omega(0)(Y-\frac{1}{2}\delta Y_{\mathrm{H}})}\delta Y_{\mathrm{H}}}{\omega''(0) Y^{1/2}(Y-\delta Y_{\mathrm{H}})^{1/2}}\right\} \times \left\{16\omega^4(0) - 16\frac{\omega^3(0)}{Y} - 16\frac{\omega^3(0)}{Y-\delta Y_{\mathrm{H}}} - \frac{36\omega^2(0)}{Y^2} - \frac{36\omega^2(0)}{(Y-\delta Y_{\mathrm{H}})^2} - \frac{12\omega^2(0)}{Y(Y-\delta Y_{\mathrm{H}})} + \ldots\right\}. \tag{A.50}$$

Taking the rapidity Y to be 19 for the LHC energy $\sqrt{s} = 14\,000\,\mathrm{GeV}$, and $\omega(\nu = 0) = 4\bar{\alpha}_{\mathrm{s}} \ln 2$, the first and second terms in the brackets of (A.50) are the largest terms, and hence at leading order

$$P^{\mathrm{BFKL}}_{\mathrm{enhanced}} = \frac{32B\pi^8}{(2\bar{\alpha}_{\mathrm{s}})^5\omega''(0)p^2} \frac{\delta Y_{\mathrm{H}}}{Y^{1/2}(Y-\delta Y_{\mathrm{H}})^{1/2}} \mathrm{e}^{2\omega(0)\left(Y-\frac{1}{2}\delta Y_{\mathrm{H}}\right)} \times \left\{(2\omega(\nu=0))^4 - 2\frac{(2\omega(\nu=0))^3}{Y} - 2\frac{(2\omega(\nu=0))^3}{Y-\delta Y_{\mathrm{H}}}\right\}. \tag{A.51}$$

References

1. Y. Dokshitzer, V. Khoze, T. Sjostrand, Phys. Lett. B **274**, 116 (1992)
2. J. Bjorken, Int. J. Mod. Phys. A **7**, 4189 (1992)
3. E. Gotsman, E.M. Levin, U. Maor, Phys. Lett. B **309**, 199 (1993)
4. E. Gotsman, H. Kowalski, E. Levin, A. Prygarin, M. Ryskin, Eur. Phys. J. C **47**, 655 (2006)
5. J. Bartels, S. Bondarenko, K. Kutak, L. Motyka, Phys. Rev. D **73**, 093 004 (2006)
6. A. Mueller, Nucl. Phys. B **437**, 107 (1995)
7. L.N. Lipatov, Phys. Rep. **286**, 131 (1997)
8. H. Navelet, R. Peschanski, Phys. Rev. Lett. **82**, 1370 (1999)
9. H. Navelet, R. Peschanski, Nucl. Phys. B **634**, 291 (2002)
10. H. Navelet, R. Peschanski, Nucl. Phys. B **507**, 353 (1997)
11. E. Levin, J. Miller, A. Prygarin, arxiv:0706.2944 [hep-ph]
12. M. Braun, arxiv: hep-ph/0504002
13. A. Bialas, H. Navelet, R. Peschanski, Phys. Lett. B **427**, 147 (1998)
14. M. Kozlov, E. Levin, Nucl. Phys. A **739**, 291 (2004)
15. H. Navelet, S. Wallon, Nucl. Phys. A **522**, 237 (1998)
16. V. Khoze, A. Martin, M. Ryskin, Phys. Lett. B **401**, 330 (1997)
17. V. Khoze, A. Martin, M. Ryskin, Phys. Rev. D **56**, 5867 (1997)
18. J. Ellis et al., Nucl. Phys. B **106**, 326 (1976)
19. T.G. Rizzo, Phys. Rev. D **22**, 178 (1980)
20. T.G. Rizzo, Phys. Rev. D **22**, 1824 (1980) Addendum
21. S. Dawson, Nucl. Phys. B **359**, 283 (1991)
22. S. Bentvelsen, E. Laenen, P. Motylinski, NIKHEF 2005-007
23. A. Mueller, B. Patel, Nucl. Phys. B **425**, 471 (1994)
24. E. Iancu, A. Mueller, Nucl. Phys. A **730**, 494 (2004)
25. E. Iancu, A. Mueller, Nucl. Phys. A **730**, 460 (2004)
26. Y. Kovchegov, Phys. Rev. D **72**, 094 009 (2005)
27. S. Bravo, I. Gallart, Eur. Phys. J. C **27**, 1 (2003)
28. J. Foreshaw, D. Ross, Quantum Chromodynamics and the Pomeron. Cambridge University Press, p 93
29. G. Altarelli, G. Parisi, Nucl. Phys. B **126**, 298 (1977)
30. V. Khoze, A. Martin, M. Ryskin, Eur. Phys. J. C **18**, 167 (2000)
31. V. Khoze, A. Martin, M. Ryskin, Eur. Phys. J. C **54**, 199 (2008)